




Publication Year	2022
Acceptance in OA	2025-02-10T11:11:34Z
Title	The EUSO@TurLab project in the framework of the JEM-EUSO program
Authors	Barrillon, P., Battisti, M., Belov, A., Bertaina, M., Bisconti, F., Blin-Bondil, S., Bonino, R., Capel, F., Caruso, R., Casolino, M., CONTINO, Giovanni, Cotto, G., Dagoret-Campagne, S., Fenu, F., Fornaro, C., Forza, R., Gorodetzky, P., Guardone, N., Jung, A., Klimov, P., Manfrin, M., Marcelli, L., Mignone, M., Miyamoto, H., Mulas, R., Onorato, M., Parizot, E., Piotrowski, L., Plebaniak, Z., Prevot, G., Szabelski, J., Suino, G., Takizawa, Y., Tibaldi, P., Vigorito, C., Youssef, A.
Publisher's version (DOI)	10.1007/s10686-022-09871-8
Handle	http://hdl.handle.net/20.500.12386/35866
Journal	EXPERIMENTAL ASTRONOMY
Volume	55



The EUSO@TurLab project in the framework of the JEM-EUSO program

P. Barrillon^{1,2} · M. Battisti^{3,4} · A. Belov⁵ · M. Bertaina^{3,4}  · F. Bisconti^{3,4} · S. Blin-Bondil^{6,7}, et al. [full author details at the end of the article]

Received: 29 January 2022 / Accepted: 16 September 2022 / Published online: 7 October 2022
© The Author(s) 2022

Abstract

The EUSO@TurLab project aims at performing experiments to reproduce Earth UV emissions as seen from a low Earth orbit by the planned missions of the JEM-EUSO program. It makes use of the TurLab facility, which is a laboratory, equipped with a 5 m diameter and 1 m depth rotating tank, located at the Physics Department of the University of Turin. All the experiments are designed and performed based on simulations of the expected response of the detectors to be flown in space. In April 2016 the TUS detector and more recently in October 2019 the Mini-EUSO experiment, both part of the JEM-EUSO program, have been placed in orbit to map the UV Earth emissions. It is, therefore, now possible to compare the replicas performed at TurLab with the actual images detected in space to understand the level of fidelity in terms of reproduction of the expected signals. We show that the laboratory tests reproduce at the order of magnitude level the measurements from space in terms of spatial extension and time duration of the emitted UV light, as well as the intensity in terms of expected counts per pixel per unit time when atmospheric transient events, diffuse nightlow background light, and artificial light sources are considered. Therefore, TurLab is found to be a very useful facility for testing the acquisition logic of the detectors of the present and future missions of the JEM-EUSO program and beyond in order to reproduce atmospheric signals in the laboratory.

Keywords Ultra-high energy cosmic rays · JEM-EUSO · TurLab

1 Introduction

The main objective of the Joint Experiment Missions for Extreme Universe Space Observatory (JEM-EUSO) program [1], is the realization of ambitious space-based missions devoted to scientific research of Extreme Energy Cosmic Rays (EECRs, $E > 5 \times 10^{19}$ eV), as well as Extreme Energy neutrinos ($\text{EE}\nu$) and ν_τ with $E > 10^{17}$ eV. The JEM-EUSO program is an evolution and extension of the original JEM-EUSO (Extreme Universe Space Observatory on board the Japanese Experiment Module) mission and inherits its observational concept [2]. Looking downward from

a Low Earth Orbit (LEO), a JEM-EUSO-like mission will identify EECRs and $EE\nu$ by observing the fluorescence emission from the generated Extensive Air Showers (EAS) during their passage through the atmosphere. ν_τ will be identified by pointing the detector towards the limb and looking at the Cherenkov emission by EAS generated by τ leptons in the atmosphere produced by ν_τ interactions in the Earth's crust. This paper focuses only on EECRs even though very similar signals would be expected from $EE\nu$. The Earth's atmosphere works as detector medium for EECRs but, at the same time, it is the main source of many other transient signals whose origin is natural, such as Transient Luminous Events (TLEs) [3], meteors, night-glow variations, and bio-luminescence, or anthropogenic, such as ground flashers and space debris, and whose spatial extension and duration are quite variable (< 1 m till ~ 100 km and from microseconds to seconds). It could even be the place to search for unknown phenomena and only hypothesized forms of matter (e.g. nucleonites [4]). All these phenomena could be considered as a source of background and disturbance for the observation of EECRs, but on the other hand they represent by themselves scientific targets. It would be, therefore, valuable to build a sufficiently flexible instrument with its main goal being the EECR and neutrino science, but at the same time, capable of contributing to the exploration and understanding of other scientific targets. The experiments of the JEM-EUSO program launched so far have already provided first results in this respect [5, 6].

The JEM-EUSO program includes several missions from ground (EUSO-TA [7]), from stratospheric balloons (EUSO-Balloon [8], EUSO-SPB1 [9], EUSO-SPB2 [10]), and from space (TUS [11], Mini-EUSO [12]) employing fluorescence detectors to demonstrate the EECR observation principle from space in view of the future large size missions K-EUSO [13] and POEMMA [14]. They all share the same concept of an optical system varying between order of 10^{-1} and 10 m² size with an angular resolution in the range 0.05 - 1 degree, and a focal surface of the order of 10^2 - 10^5 pixels, either with Multi-Anode Photo-Multiplier Tubes (MAPMTs) or/and Silicon Photo-Multipliers (SiPMs).

The main task of the Data Acquisition (DAQ) chain and in particular for the trigger system is to deal with the highly variable conditions of the atmosphere which might induce an excessive spurious trigger rate, well above the sustainable one. The possibility to reproduce at some extent in laboratory the various atmospheric conditions that the detector would observe from space is very much beneficial as it would allow to cross-check and refine the acquisition logic, avoiding to discover possible inefficiencies or malfunctionings while in space.

Originally developed in the contest of the JEM-EUSO mission, the core objective of the EUSO@TurLab project [15] is to test the electronics and trigger system of the different detectors of the JEM-EUSO program in quasi-real conditions in terms of light intensity, as well as spatial and temporal light variations. The use of the TurLab tank allows reproducing experimentally variable light conditions, recreating orbit sights and events as expected to be seen by the JEM-EUSO mission and by the projects of the JEM-EUSO program. For this reason in the following the term JEM-EUSO will refer to both the program and the mission, if needed it will be specified. The experiments performed at TurLab were designed based on simulation results of the expected light signals seen from space. Thanks to the experimental

data retrieved by TUS and more recently by Mini-EUSO, it is now possible to compare them with those collected at TurLab to understand at which level of fidelity they reproduce the actual observations from space. It is important to emphasize that it is out of the scope to reproduce exactly the natural and artificial phenomena as seen from space as we can not completely reproduce all of the Earth's atmospheric phenomena. What matters the most is the capability of reproducing them at least at the order of magnitude level in terms of temporal duration, spatial extension and luminous intensity. This is important because it validates the concept of the EUSO@TurLab project and, if needed, refine the future tests in order to emulate even more precisely the specific signals expected in space. Moreover, the TurLab facility can be used to test on ground upgraded acquisition firmware with high reliability prior to implement them on-board satellites or balloons with a significant resource saving.

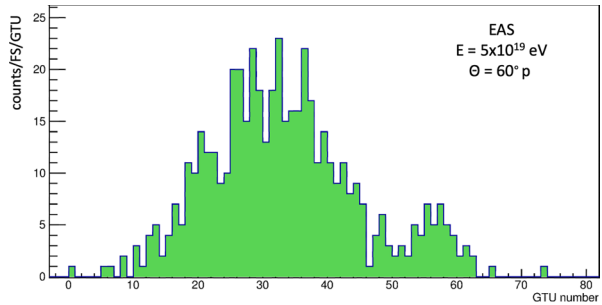
The paper is organized as follows. Section 2 summarizes the main characteristics of the space-based missions of the JEM-EUSO program including the original JEM-EUSO mission. Section 3 describes the TurLab facility and the phases of the EUSO@TurLab project with the different setups used to emulate UV transients. Section 4 compares in details the signals reproduced at TurLab with those in space focusing on: a) light intensity and variation from diffuse sources; b) spatial and temporal evolution of the signals from urbanized areas, meteors, lightning, flashers and EAS. Section 5 describes experiments conducted at TurLab regarding other applications such as remediation of space debris and ocean studies, and reports on campaigns performed with instrumentation of the JEM-EUSO program. Perspectives and conclusions are subject of Section 6.

2 Summary of the JEM-EUSO detectors

One of the observational principles of a space-based instrument aiming to investigate EECRs science is based on the detection of the UV (300 - 430 nm) fluorescence photons produced along the track of EASs in the atmosphere. These signals last typically between 50 - 150 μ s and extend on tens of kilometers in size depending on the zenith angle of the EAS. Due to the fact that EECRs above 5×10^{19} eV have a flux lower than 1 event per century per square kilometer [16], huge exposures are necessary to collect sufficient statistics. As an example, the accumulated exposure by the Pierre Auger Observatory (PAO) in 15 years of operation between 2004 and 2018 for the measurement of the cosmic ray spectrum above 2.5×10^{18} eV amounts to slightly more than 60,000 $\text{km}^2 \text{sr yr}$ (the nominal annual exposure of PAO being order of 10 times smaller taking into account that the apparatus has grown in size along the first years of operation) [16]. This value corresponds to the expected annual exposure by the JEM-EUSO mission [17].

Moreover, the detector should have good enough temporal and spatial resolutions to properly image the event and reconstruct the track. Figure 1 shows an example of an expected light profile of a 5×10^{19} eV proton EAS with zenith angle 60° simulated with the EUSO Simulation and Analysis Framework (ESAF) code [18] for the JEM-EUSO mission. In the following, the most relevant parameters of the original JEM-EUSO telescope are briefly mentioned to provide some references. A more

Fig. 1 Light profile of a 5×10^{19} eV proton EAS with zenith angle 60° simulated with the ESAF code [18]. The vertical axis indicates the detected photo-electron counts per data frame (GTU, see text for the definition) on the full Focal Surface of the JEM-EUSO mission



detailed description of the mission, its aims, detection strategy and expected performance is reported in [2].

The JEM-EUSO telescope is conceived with a Field-of-View (FoV) of ~ 0.85 sr orbiting on-board the International Space Station (ISS). The optics is composed of three Fresnel lenses with a 4.5 m^2 optical aperture. The telescope records the EAS-induced tracks with a time resolution of $2.5 \mu\text{s}$ (Gate Time Unit; GTU). The Focal Surface (FS) detector is formed by 137 Photo Detector Modules (PDMs) composed of ~ 5000 MAPMTs in total (36 MAPMTs per PDM, 64 pixels each). The FS detector is highly pixelated in $\sim 3 \times 10^5$ channels providing a spatial resolution of $\sim 0.074^\circ$, equivalent to $\sim 0.55 \text{ km}$ at ground seen from an altitude of $\sim 400 \text{ km}$. An optical filter is placed in front of each MAPMT to select photons in the fluorescence bandwidth. Since the ISS orbits the Earth in the latitude range of $\pm 51.6^\circ$, moving at a speed of $\sim 7.7 \text{ km s}^{-1}$, the variability of the FoV observed by JEM-EUSO is much higher than that observed by ground-based experiments. Indeed, the pixel-FoV changes completely every $\sim 70 \text{ ms}$. Moreover, making ~ 15.5 orbits per day, every 45 minutes on average the ISS has a transition between day and night regions. In reality, the illumination period depends on the β angle of the ISS, which is the angle between the orbital plane of the station and the Sun-Earth vector. Therefore, the night and day portions of the orbit significantly differ depending on the period of the year.

Along the years, the JEM-EUSO concept has evolved in a short- and long-term development program with different missions from ground, balloon and space-platforms with different complexity and objectives. Namely, the JEM-EUSO mission itself could not be realized. The EUSO-TA on ground and the missions on balloons aim to develop and test the key elements of the JEM-EUSO concept, in order to raise their technological readiness level and demonstrate the fluorescence technique from suborbital altitudes. The TUS and Mini-EUSO telescopes are designed to serve as path-finder and/or small scale missions for the K-EUSO and POEMMA middle and large class missions. Table 1 provides a summary of the main parameters of the different space telescopes within the JEM-EUSO program, which are of relevance for the EUSO@TurLab measurements. Due to the totally different flight speed of stratospheric balloons, typically 2 - 3 orders of magnitude slower than space missions in Low Earth Orbits, replicas of flight paths of EUSO-SPB can not be reproduced with the same fidelity as for the space projects. However, in some cases this is not

Table 1 Approximated values for the typical parameters of the different space missions of the JEM-EUSO program

Parameter	JEM-EUSO	TUS	Mini-EUSO	K-EUSO	POEMMA
Orbital height (km)	400	480	420	400	525
Orbital speed (km/s)	7.7	7.6	7.7	7.7	7.6
Pixel FoV (deg)	0.075	0.6	0.9	0.11	0.084
Pixel FoV at ground (km)	0.55	5	6.5	0.8	0.76
Full FoV (km)	460	80	340	290	435
Pixel FoV duration (ms)	72	660	860	130	100
Optics size (m ²)	4.5	2	0.05	5	6
Time resolution (μ s)	2.5	0.8	2.5	1	1

an issue. As an example, if the main purpose of the tests is to verify that the trigger thresholds are adjusted fast enough in time to follow the variations of the light intensities at pixel level induced by the relative speed between the detector and a fixed light source on ground, then a positive result on a test performed by simulating space orbits is a guarantee that the trigger logic will satisfy the requirements also for balloon speeds.

3 The EUSO@TurLab project and relative development phases

TurLab is a laboratory, equipped with a 5 m diameter rotating tank, located at the Physics Department of the University of Turin (see Fig. 2) (<http://www.turlab.ph.unito.it>). The system has been conceived mainly for studying fluid-dynamics problems where system rotation plays a key role in the fluid behavior, as it happens in atmospheric and oceanic flows at different scales.

The tank can be filled up to 70 cm with water (both fresh or salty) and can rotate with periods that span from about tens of seconds to ~ 20 minutes. For fluid-dynamics experiments the facility is equipped with cameras and an advanced system for digital recording and data processing. The TurLab facility is located 15 m underground. Therefore, it is possible to work in extremely dark conditions and hence the light intensity in the room can be varied by researchers.

The tank can be used in various settings, which allow the study of different atmospheric phenomena. A few examples are: a) it can be filled with fluids of different density to study fluid behaviour in stratified conditions both with or without rotation; b) convection can be generated and studied with different approaches; c) two fans can create an air flow, between about 1 and 7 m/s, that induce waves on the fluid surface, which allow the study of the air-water interaction or/and create conditions of infinite fetch that can be deeply analyzed with fluid-dynamics techniques or with two waves probes; d) the possibility of different surface roughness allows studies of fluid turbulent properties in the boundary layer; e) the facility can be used as a model of the rotating Earth system to simulate parts of terrestrial surface by

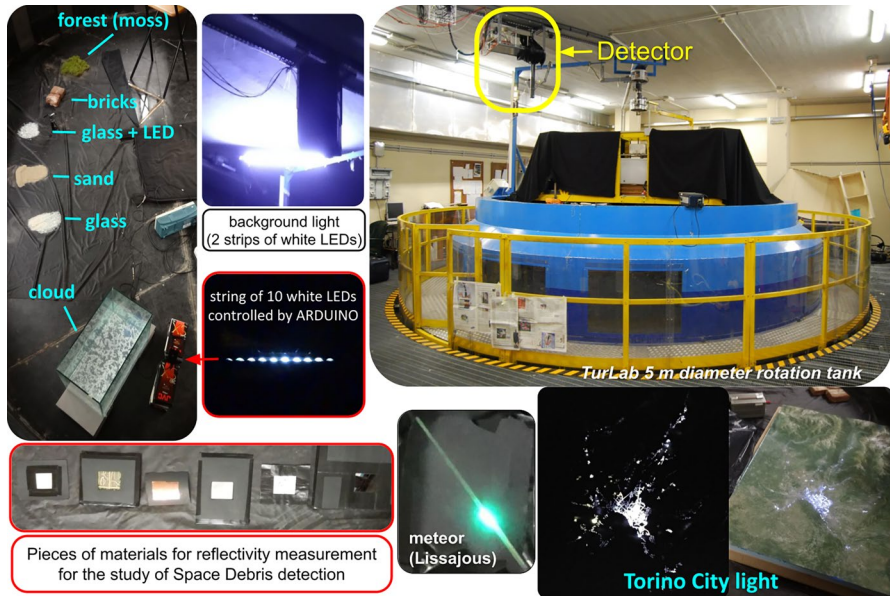


Fig. 2 TurLab tank (right-top) setup with the EUSO@TurLab detector hung on the ceiling, light sources and materials to reproduce atmospheric phenomena that a detector in space can observe. Bottom left side shows examples of materials which might become space debris (see Section 5 for details). Right bottom part of the figure shows a reproduction of the city of Turin which is used in the experiments at TurLab to mimic city lights (see text for further details)

reproducing different environments using water (ocean, fog and clouds) and without water (snow, grass, land) and their albedo.

To realize an emulation of observations from the ISS, the TurLab rotating tank is used with a series of different configurations to recreate the Earth views, and the EUSO@TurLab apparatus is hung on the ceiling above the tank pointing towards the nadir to emulate a JEM-EUSO telescope [19].

Within the EUSO@TurLab project the tank is equipped with light sources which are essentially of two kinds: a) direct light emitting sources; b) materials reflecting room light as can be seen in Fig. 2. The different types of sources employed at TurLab are summarized in the following.

- A diffused background light is produced by a high power LED lamp suspended on the tank structure and pointing towards the ceiling. The intensity is controlled by a DC power supply, which can be adjusted either statically or dynamically depending on the targeting conditions to be reproduced.
- A replica of the Turin region to emulate artificial lights from cities, villages and roads. The light intensity can be controlled and varied either by varying the applied voltage to LEDs or by removing or adding sheets of glass paper which cover the LED stripes to diffuse the emitted light.
- LEDs driven by a pulse generator, and/or smashed glass illuminated by LEDs for fast luminous events such as lightnings. The role of the smashed glass is to

produce non uniform light emission in different points and directions. A variety of signals is generated by changing the intensity and repetition time of the pulsed LED.

- An oscilloscope producing Lissajous curves, for events such as meteors. With this technique linear tracks of different time duration (> 100 ms - ~ 2 s) and speed can be easily generated. The phosphorescent signal on the oscilloscope mimics the meteor trail. The intensity of the phosphorescent light can be varied to emulate meteors of different magnitudes.
- LEDs and optical fibers driven by an Arduino (<http://www.arduino.cc>) board to control light sources with very short timing (3μ s) or to recreate complicated luminous phenomena, such as ELVEs [20] (Emission of Light of Very low frequency perturbations due to Electromagnetic Pulse sources). By changing the impedances of the circuit the light intensity emitted by the LEDs is controlled. Till now EECRs are recreated with a strip of 10 LEDs. ELVEs are reproduced with optical fibers arranged in a quarter circle and illuminated by LEDs.
- The tank is covered by a black fabric to reduce the light diffusion within the nominal range expected from space in case of the experiments of the JEM–EUSO program, typically ~ 1 count/pixel/GTU, but it can vary a few times among different points of the tank due to the presence of a permanent bridge across the tank and other structures that impede a uniform diffusion of the light inside the tank. The count rate here indicated has to be considered only as a reference value. The airglow is a variable process in space and time typically within a factor of ~ 3 in absolute counts [21]. The clouds usually increase the light intensity within a factor of two [21, 22], the exact amount depends on the cloud characteristics (i.e. height and optical depth). The background light increase by effect of moon light varies within a range of 30 between new moon and full moon conditions [17]. Moreover, ISS orbits show large variations of light intensity depending on the reflecting surface on ground or in atmosphere and due to the presence of natural or artificial lights. The non uniform light emission is suitable to test the good adaption of the trigger logic to variable background conditions.
- Different materials are used to obtain variations in the intensity of the reflected light inside the tank: moss, sand, bricks, glass dust, mirror. The first three recall forests, deserts, and savannah regions. The reflected light is only moderately different from the black fabric. Glass dust and mirror provide a much more intense light reflection to artificially create large variations in the reflected light from the black fabric. These two materials can recall some part of the Earth's surface with higher reflectance such as snow, glacier and calm lake or ocean.
- By switching OFF the high power LED lamp illuminating the ceiling, the count rate decreases by orders of magnitude. This is used to mimic specific acquisitions in Mini-EUSO (see Section 4.1 for details).
- A cloud-like scenario is created using a small container placed inside the tank filled with 2-3 layers of water with different salt concentrations and layers of suspended particles to reproduce examples of cloud albedo and cloud diffusion. Depending on their concentration, particles can coalesce in a single wide layer or they can form puffy clouds providing different average reflection. This is the same methodology used in fluid-dynamics experiments at the tank [23].

Moreover, by placing a steady light source below the transparent container a diffusive situation like city lights in a cloudy night can be reproduced.

The tank has been used also with the following configurations for specific fluid-dynamics and space debris related tests:

- The tank is filled with 70 cm of water and industrial fans are used to generate sea waves. A lamp illuminates the water and the reflected light is retrieved by the EUSO@TurLab apparatus. Inside the tank, water dedicated probes measure the amplitude of waves. This is used to verify the capability of detecting waves under the assumption, that needs to be verified from space, that the UV albedo is different in calm or rough sea conditions due to the fact that higher waves increase the chance to produce a more specular surface that directly reflects part of the light to the sensor (see Section 5 and Fig. 25 for details).
- The tank is filled with water and patches of foam produced with commercial soaps and detergents are used to study the variations of albedo in view of studying ocean phenomena.
- An Aluminum-ball is attached at the end of a stand which is fixed at the bottom of the tank. A powerful LED shines the Aluminum-ball from outside the tank. The reflected light hits the sensor and mimics the albedo of Space Debris (SD) illuminated by the sun (see Section 5 and Fig. 26 for details).
- Different materials such as polished aluminum foil, canned aluminum, unpolished aluminum foil, mirror, copper foil, white paper, a ball of Aluminum foil, a sample of Kevlar, electronics board (see bottom left Fig. 2), which often compose SD, are placed on the bottom of the tank, within the FoV of the EUSO@TurLab apparatus, in order to measure the relative reflectances of these materials in view of SD studies.

Data taking is organized in sessions and between sessions the setup has to be dismantled to allow fluid-dynamics experiments. Therefore, the light intensity and the distribution of the various light sources are not perfectly reproducible among sessions. Moreover, along the years the system has evolved to perform specific tests. Consequently, results might vary between sessions even within a factor of a few if they are within the range to mimic JEM–EUSO observations. Otherwise, a more detailed fine tuning is performed at a level of tens of percent if specific needs require it. Figure 3 shows a typical configuration of the tank setup during one session of data taking.

Regarding the EUSO@TurLab apparatus itself, different detectors and readout-electronics setups have been adopted along the years, all using a 1-inch lens as optical system. The typical focal lengths used in our system vary between 30 and 50 cm. Taking into account that the pixel pitch is ~ 3 mm, the angular resolution is of the order of $0.3^\circ - 0.6^\circ$.

High Voltages (HV), DC power supplies, function generators and monitoring oscilloscopes are on the desk by the side of the tank with a PC with LabView (<https://www.ni.com/it-it/shop/labview.html>) interface. They are used to power the EUSO@TurLab apparatus, pilot the different light sources and monitor the

Typical TurLab Tank Setup

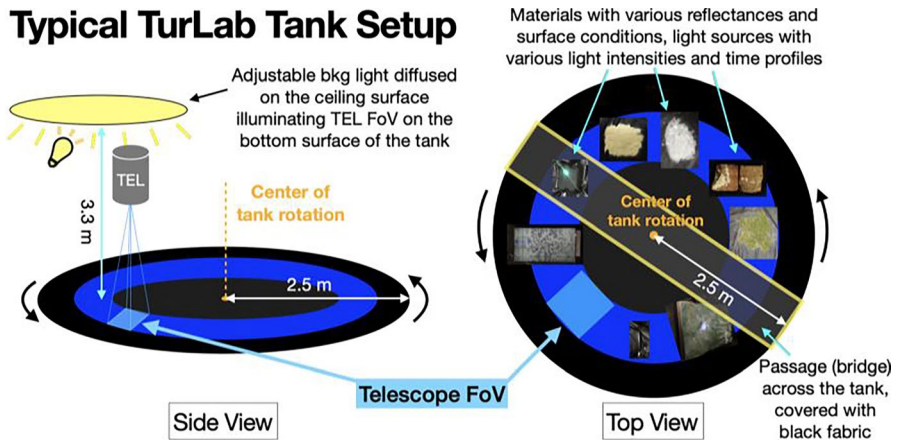


Fig. 3 Typical TurLab tank setup during a session of data taking (TEL=telescope and bkg=background)

apparatus response and data acquisition. ROOT (<https://root.cern>) and ETOS [24] software are used for monitoring and analysis.

The capability of changing the rotation speed of the tank gives the opportunity of producing slower and faster light transitions (within a factor of ~ 20) adapting the experiment to the intended situation. In general, the fact that the tank can be rotated with periods reaching 20 minutes allows reproducing entire night orbits or significant portions of them. The possibility of controlling light illumination allows recreating moonrise and moonset, or day and night transitions. On the other hand, to simulate the residence time of point-like sources in the FoV of a pixel, it is important to reproduce similar angular speed as seen from orbit. To be considered as a point-like source in the JEM-EUSO-like detector, the light source should have an extension smaller than the pixel FoV. It corresponds, therefore, to less than 500 m in JEM-EUSO and less than 6 km in Mini-EUSO. Similarly, at TurLab it corresponds to less than 1 - 2 cm on the tank floor depending on the optical system adopted in the measurements. Moreover, considering the limited FoV of the TurLab setup ($< \pm 5$ deg from nadir), a uniform emission in all directions by the LED can be assumed. Table 2 shows a few examples of rotation speeds in order to obtain two extreme cases: JEM-EUSO and Mini-EUSO configurations (see Table 1).

Along the years, different types of electronics read-out were used, improving step by step the capability to replicate the on-board measurements and the EUSO@TurLab apparatus has gone through three different phases.

3.1 Phase I

The EUSO@TurLab apparatus used in the first phase (2010 - 2014) [25] consists of a 5×5 pixels MAPMT: Hamamatsu R8900-M25 [26], hung from the ceiling and pointing towards nadir; 25 cables, 25 m long, connecting each pixel of the MAPMT with the electronics; standard NIM and CAMAC electronics and a PC for acquiring measurements with LabView.

Table 2 Rotation speed of the tank to reproduce the equivalent transition time of a point-like source in the FoV of one pixel for the JEM-EUSO and Mini-EUSO cases taken as the two extreme conditions of Table 1

Instrument	Time to change pixel FoV (ms)	Rotation period of TurLab (s)	
		30 cm FL	50 cm FL
JEM-EUSO	72	54	90
Mini-EUSO	860	640	1060

In the following it has been assumed that the light source is located at 2 m distance from the lens of the EUSO@TurLab apparatus and that it is positioned close to the edge of the tank where the circumference is ~ 15 m. The two cases of 30 cm and 50 Focal Length (FL) are considered

The electronic system is very different from the JEM-EUSO one, although it is based on the same detection principle of the single photon-counting (see Fig. 4). With this setup it is not possible to reproduce the JEM-EUSO time scale, with a GTU of $2.5 \mu\text{s}$ and a 25 ns double-pulse resolution (which is the one expected for JEM-EUSO). Therefore, 400 ns double-pulse resolution and $40 \mu\text{s}$ GTU are adopted to keep the same maximum number of measurable photo-electron counts per GTU as in JEM-EUSO. A very unwanted feature of such an electronics configuration, which is resolved in the latest phases is the delay in the PC acquisition: 30 ms dead time for each measurement. Hence, for EUSO@TurLab, 1 GTU consists of $40 \mu\text{s}$ sampled every 30 ms. The acquisition with this configuration, therefore, is dominated by dead-time. However, Phase I helped in fine tuning the intensity of the different light sources, also in view of much shorter GTUs, and it demonstrated the general feasibility of the EUSO@TurLab concept. Moreover, at that time there was no online implementation of the trigger logic. The trigger response was emulated offline. Therefore, the issue of the dead-time was mostly circumvented by slowly rotating the tank or test light sources in static conditions (i.e. Arduino circuits, meteors).

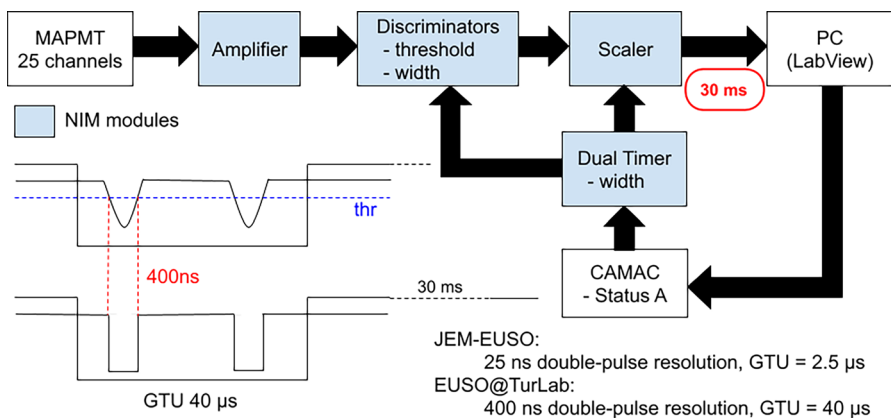


Fig. 4 Electronic setup of Phase I at TurLab. See text for details

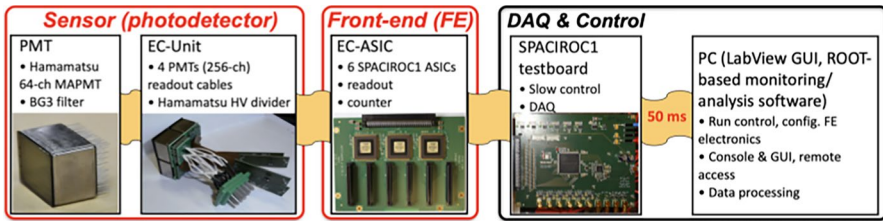


Fig. 5 Electronic setup of Phase II at TurLab. See text for details

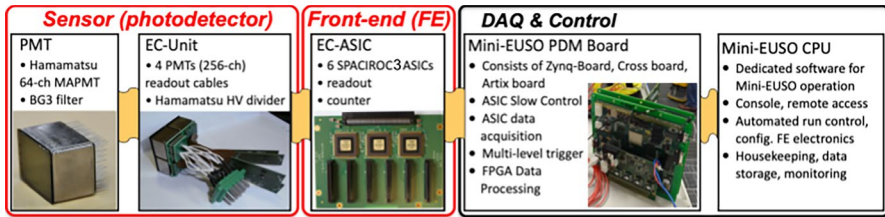


Fig. 6 Electronic setup of Phase III at TurLab. See text for details

3.2 Phase II

The instrumentation used in the second phase (2015 - 2017) [27] is upgraded compared to the first phase by using an Elementary Cell (EC) unit (4 MAPMTs, 64 channels each) and the readout by the JEM-EUSO front-end electronics with an ASIC evaluation board [28] (see Fig. 5). The main improvement of this configuration consists in collecting data with $2.5 \mu s$ resolution by means of the JEM-EUSO instrumentation. However, the data readout introduces a 50 ms dead time between blocks of 128 GTUs of data, named packets in the following. The trigger configuration is not implemented either. This is the electronics used at the time of the EUSO-Balloon flight and of the installation and first campaigns of the EUSO-TA telescope. The data acquired at this time were used to fine tune the First Level Trigger (FLT) of JEM-EUSO mission and its adaptations for ground and balloon experiments [29].

During the latest part of Phase II TurLab hosted sessions of data taking to test the elaborated FLT trigger logic and evaluate its performance in view of the EUSO-SPB1 mission. For these sessions the PDM that flew on EUSO-Balloon was employed as a detector and the trigger configuration was implemented in FPGA.

3.3 Phase III

In the third phase (since 2018) [30, 31] a significant change in the read-out electronics is applied (see Fig. 6), which is the one employed in the Mini-EUSO

configuration that records data with different time resolutions ($2.5 \mu\text{s}$, $320 \mu\text{s}$, and 41ms). With this configuration, no dead time exists between acquired data at 41ms time resolution (D3 data). In parallel, it is possible to acquire up to 4 packets of data with $2.5 \mu\text{s}$ (D1 data) and $320 \mu\text{s}$ (D2 data) time resolutions, every 5.24s . This configuration is shown in Fig. 7. During this phase, the Mini-EUSO Engineering Model (Mini-EUSO EM) was tested as well (2018) to check the DAQ and trigger performance [32] (Fig. 26).

All along the different studies described in this paper, unless differently mentioned, the conventional GTU used in the plots is the shortest time unit adopted in the acquisitions which is $2.5 \mu\text{s}$ for second and third phases, and $40 \mu\text{s}$ for the first phase.

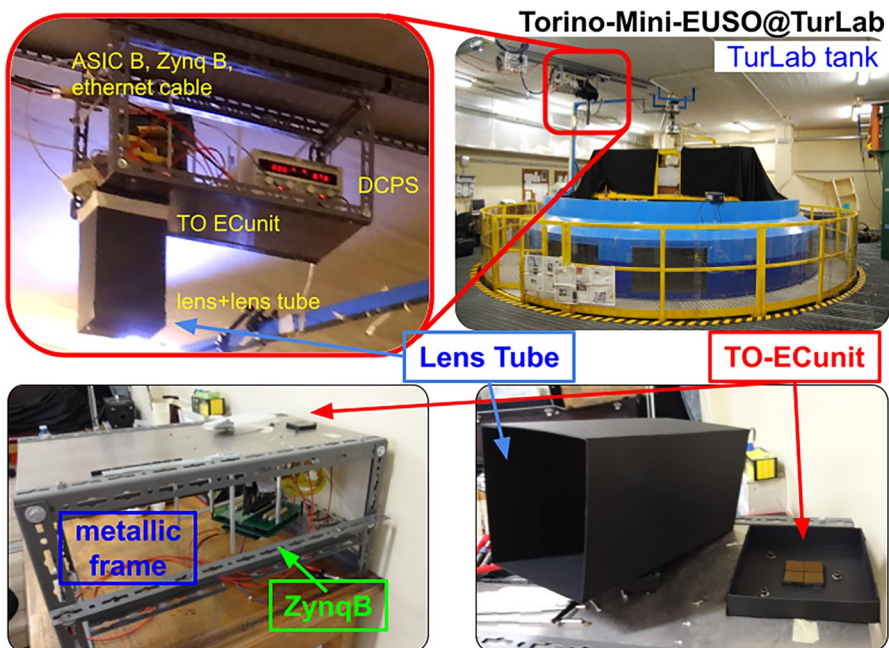


Fig. 7 The EUSO@TurLab configuration in the third phase consists of a lens tube with a 1-inch plano-convex lens, an EC unit, front-end electronics based on SPACIROC3 ASICs, the Zynq board connected to a PC via ethernet cable, where the CPU software, a dedicated software for Mini-EUSO data processing system, is installed. Electronics boards and MAPMTs are powered by external low and high voltage power supplies (DCPS), respectively. A metallic frame is used to hold the experimental setup and to fix it on the ceiling

4 Comparison between TurLab measurements and space observations

Thanks to the data collected by Mini-EUSO and TUS it is possible to compare the measurements obtained with the replica at TurLab to the data acquired by the experiments, in order to understand at which level of similarity the light intensity and light profiles are reproduced with EUSO@TurLab. A first overall comparison can be done by looking at the data collected in typical orbits at TurLab using the electronics setups employed in the three different phases as summarized in Section 3 (see Figs. 8, 9, 10, and 11) with those published by Mini-EUSO [6] (see Fig. 12).

Figures 8 and 9 show measurements taken during the first phase. The MAPMT photo-electron counts (sum of counts from 25 pixels) during a complete 10 minute long rotation of the tank are shown. Different configurations are reproduced as explained in the following. In Fig. 8, the room light is the same for the two curves, with the LED over the tank switched ON. The green curve refers to the tank without any source on it, while the blue one represents the tank covered with a collection of different materials and direct light sources. In Fig. 9, the two curves refer to different room light conditions with the tank covered with all the sources shown in Fig. 8. The LED over the tank is ON or OFF in blue or green curve, respectively. As predictable,

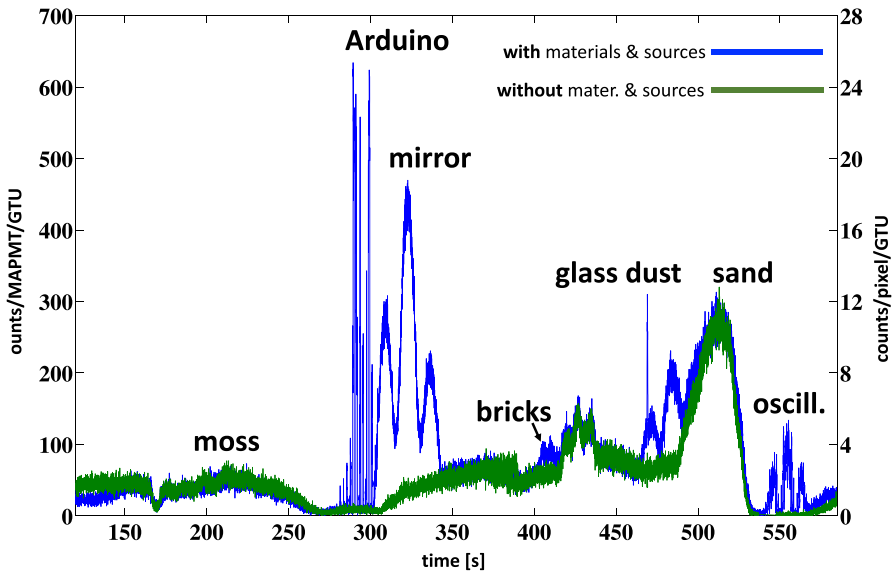


Fig. 8 A 10 minutes long rotation of the tank equipped with different sources: moss, Arduino 10 LED strip, mirror, bricks, glass dust, sand, and oscilloscope. The sum of the 25 pixels (Phase 1) is indicated on the left side of the vertical axis, while the right side shows the average count rate per pixel. The green curve refers to the tank without any source in it, while the blue one represents the tank covered with a collection of different materials and direct light sources. The unexpected response of the sand is due to the fact that it was placed in a region of the tank which is particularly bright when the LED on the tank is ON as it can be seen from Fig. 9

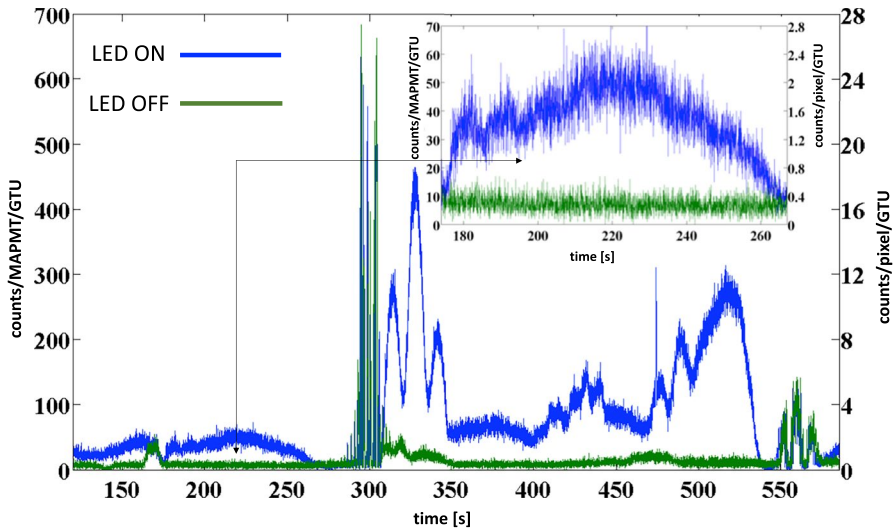


Fig. 9 Response to different light room conditions with materials inserted as in Fig. 8 (Phase 1). The LED over the tank is ON or OFF in blue or green curve, respectively. A portion of the plot is zoomed in the inset to better appreciate the count level with LED OFF. See text for details

when light emitting sources are in the FoV of the EUSO@TurLab apparatus, there is no difference between the detected light when the LED over the tank is ON or OFF. On the other hand, there is a fundamental change in the response of different reflecting materials. The inset in Fig. 9 is a zoom showing the minimum level of luminosity obtainable at TurLab which is present in different positions inside the tank, with different materials on it. An average value of 0.3 counts/pixel/GTU is obtained with LED OFF. With LED ON the typical value is around 2 counts/pixel/GTU. These are all different levels of ‘background’ light that can be used to check the sensitivity to the detection of EAS-like events by the trigger system.

The top panel of Fig. 10 shows the result of UV intensities in a full rotation of the tank with various materials during the second phase campaign when a JEM-EUSO EC unit is employed. The plot shows the summed counts of a MAPMT (= 64 pixels) as a function of time in GTUs. An average value of 0.5 - 2 counts/pixel/GTU is obtained depending on the portion of the tank in the FoV without emitting lights. It is important to note here that to obtain similar background levels between Phases I and II the light intensity in Phase II should be ~ 16 times stronger than in Phase I to compensate the much shorter integration time ($2.5 \mu\text{s}$ GTU compared to $40 \mu\text{s}$ GTU of Phase I). This also means that with light OFF the typical count rate decreases to ~ 0.02 counts/pixel/GTU in Phase II.

The middle and bottom plots concern one of the typical analyses performed on the data, which is the evaluation of the FLT performance, the JEM-EUSO one in this specific case. The FLT looks for a signal excess above the background fluctuations in a box of 3×3 pixels. To be considered as an excess the signal should stand a few standard deviations above the average background level. The pixel photo-electron counts in excess are integrated for 5 consecutive GTUs within the

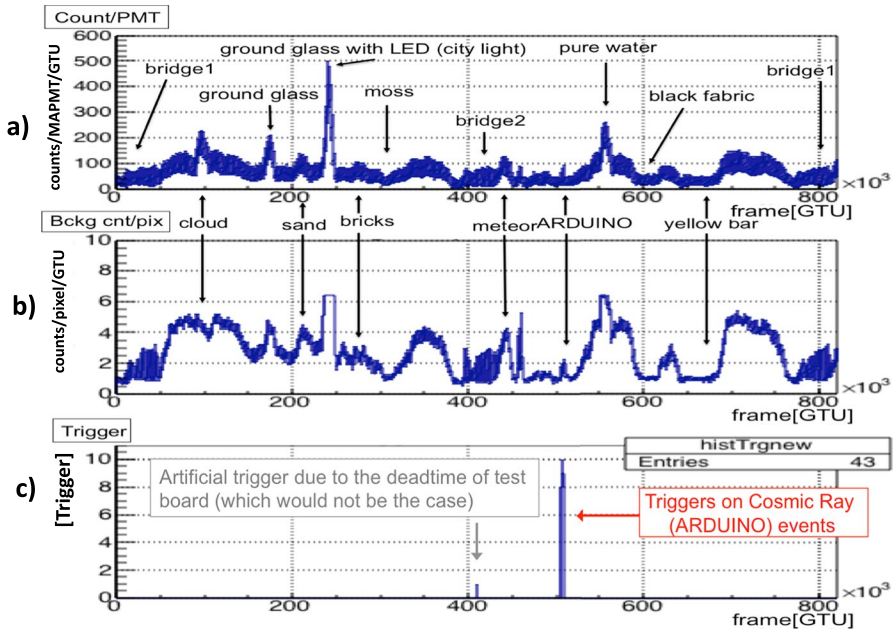


Fig. 10 The panel a) shows the raw data (counts/MAPMT, 64 pixels, Phase 2), while panel b) shows the corresponding background level which is used to set the threshold for the FLT and panel c) shows the result of the FLT, as a function of frame number (GTU = 2.5 μ s), respectively. We obtained 100% trigger efficiency for EAS-like events. A few triggers at around frame 410,000 are due to the 50 ms of dead time among packets, which would not be the case of actual JEM-EUSO observation operated with the PDM board with no dead time. The re-adjustment of the trigger thresholds, which is obtained by re-calculating the average measured background level per each pixel every 320 μ s, would have prevented the trigger to occur

3×3 pixel box. If the total excess in the pixel box is above a certain threshold, a trigger alert is issued. A counter checks that the trigger alert lasts a number of GTUs compatible with an EAS development in atmosphere (<72 GTUs) to avoid triggers on much slower events. Every 320 μ s the average background level per pixel is calculated and the threshold is updated using a common threshold for all pixels belonging to the same MAPMT. The threshold is set basing on the pixel with the highest count rate. The specific number of standard deviations and the signal excess are trigger parameters that are defined at start run. In this way it is possible to cope with fast variations of the light intensity. A more detailed description of the trigger logic can be found in [29]. The middle panel shows the averaged counts per pixel which is used to set the FLT threshold, while the bottom shows when FLT's are issued based on signals in that MAPMT, as a function of GTU. Almost all triggers coincide with passing over the Arduino driven LED chain, which emulates EAS-like events, as expected. A typical Arduino event can be found in Fig. 19 to be compared with an expected light profile by a 5×10^{19} proton EAS detected by JEM-EUSO displayed in Fig. 1. Only one trigger is not associated to an EAS-like event. Instead, it is due to a specific location near one

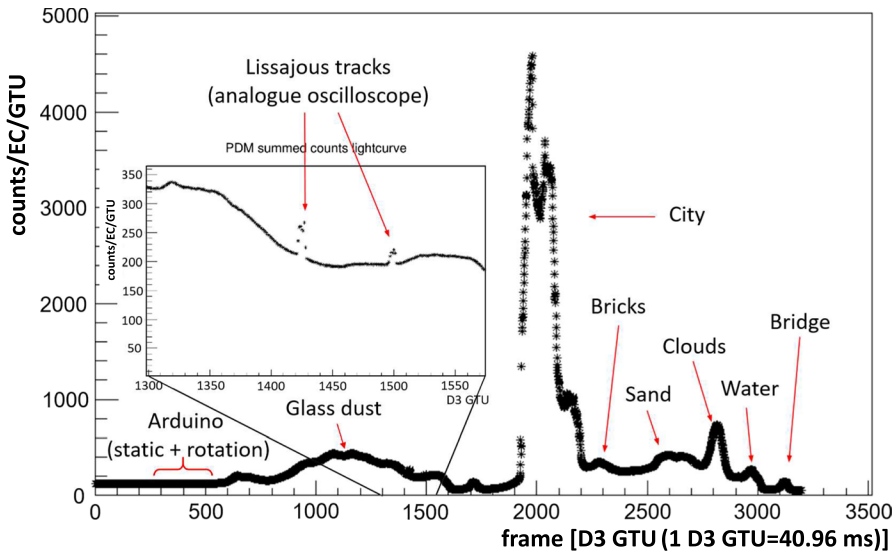


Fig. 11 Light curve of D3 data for a whole tank rotation with a speed of 2 min/rot (Phase 3). All the reflections from materials in the FoV are recorded as a continuous “movie” in D3 data while D1 and D2 stores only the events that they are targeting to trigger in their own time resolution (up to 4 events per D3 packet). Counts are renormalized to D1 GTUs. Figure adapted from [32]. See text for details

part of the bridge that crosses the tank. In this location the variations of light reflection are too fast. As the FLT logic is run offline, 50 ms of dead time among packets impede to collect data continuously during such a fast light transition and the trigger logic is not able to properly re-adjust the thresholds in due time. In other words, even though the online logic foresees a threshold update every $320 \mu\text{s}$, in reality due to the deadtime among packets, the thresholds are updated only every $\sim 50 \text{ ms}$. This is one of the essential tests that validated the trigger logic prior to the EUSO-SPB1 flight.

Figure 11 shows the emulation of one orbit taken during the third phase with the latest electronics configuration. The sum of 256 pixels is shown (one EC unit). In this case it is possible to collect data at three different sampling times. There is no dead time for D3 data. This is the closest configuration to the data taking in orbit with Mini-EUSO. The typical counts are between 0.3 and 1.5 counts/pixel/GTU.

4.1 General comparisons with Mini-EUSO observations

A few general considerations on the comparison of the light intensities recorded at TurLab in the different phases and by Mini-EUSO as shown in Fig. 12 are reported in the following. They can be easily done due to the relatively large surface area of the emitting sources. For more circumscribed areas a more refined comparison is needed.

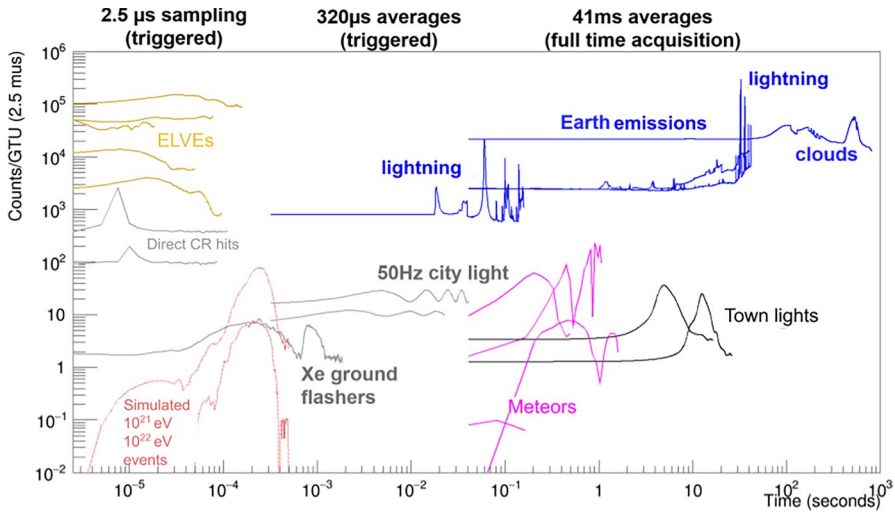


Fig. 12 Temporal profile of various signals observed by Mini-EUSO and detected at different time scales. The fastest sampling rate ($2.5 \mu\text{s}$, D1 data) allows detecting EAS-like events, ELVEs and other fast phenomena. The averaged sampling can be used to characterize slower events such as lightning, meteors, UV emissions of artificial and natural origin. The different integration time between $320 \mu\text{s}$ (D2) triggered data and the continuous data taking at 41 ms (D3 data) allows to recognize in the D2 data the typical 50 Hz city light emission which is washed out when the 41 ms data integration is adopted. The different temporal scale of towns and cities reflects the allocated time span of each D2 and D3 data packet. All curves refer to experimental data from ISS altitude except the light curves of EECRs which come from ESAF simulations. The temporal profiles are relative to the number of pixels involved in the phenomena. As an example, clouds and Earth emissions express the counts integrated on the full PDM. Further details on Mini-EUSO acquired data can be found in [6] where this image is adapted from

1. The typical background level in Mini-EUSO is around 1 count/pixel/GTU (see Mini-EUSO count rate in the first part of the ‘Town lights’ temporal profile in Fig. 12). It can vary by a factor of two or more depending on the viewed surface (ground, sea, grass, etc.) and on the pixel response. The values reproduced at TurLab, where different materials are used to change the albedo, are in agreement with these intensities as they vary typically between 100 - 500 counts/EC/GTU which correspond to 0.4 - 2 counts/pixel/GTU.
2. In presence of clouds the light intensity in Mini-EUSO increases by a factor of $\sim 2 - 3$ and this is well reproduced at TurLab where clouds increase the light signal by a similar amount.
3. By switching the lights OFF the background level is reduced to similar conditions recorded by Mini-EUSO when the HV protection system is activated and the MAPMT efficiency is reduced by 1 - 2 orders of magnitude (see Fig. 22 for a more detailed comparison). In fact, Mini-EUSO is equipped with a HV protection system that reduces by orders of magnitude the collection efficiency of the MAPMTs when the light intensity exceeds ~ 100 counts/pixel/GTU. This is done by changing the voltage set at photo-cathode level. The setup at TurLab is not provided with such a safety mechanism.

- Light intensities of cities in the Mini-EUSO data are typically 10 – 100 times brighter than the pedestal level. Similar results are obtained at TurLab, where ‘city’ light is 5 - 30 times brighter than the typical room light reflection by the bottom of the tank.
- LED pulses and glass dust can reproduce intense spikes with short duration (see Fig. 8) that can mimic lightnings as detected by Mini-EUSO.

These comparisons indicate that strong light intensities and the overall standard brightness levels are replicated in all three phases of the project typically within a factor of ~ 2 -3. Along the years, the major improvement is related to the acquisition system which became more and more representative of the electronics system in flight. Nevertheless, since its setting up EUSO@TurLab has been conceived at a reasonable level of fidelity with typical observations from space.

It is important to underline here that Mini-EUSO has been designed in such a way to detect similar photo-electron counts per pixel as in JEM-EUSO in case of diffuse light sources to test the electronics response in conditions which are as similar as possible to what was expected for JEM-EUSO. This is done by compensating the $\sim 10^{-2}$ times reduction of the optics aperture with $\sim 10^2$ times wider pixel FoV.

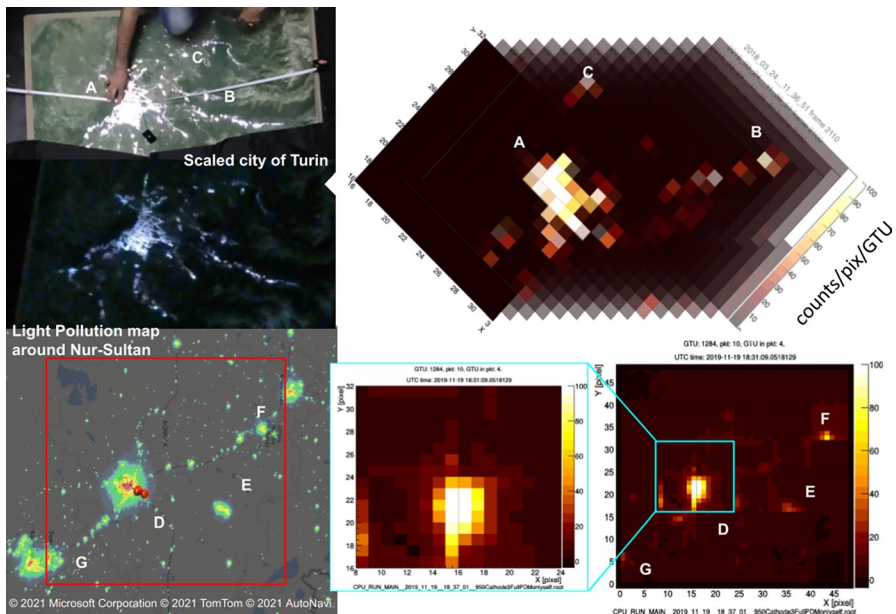


Fig. 13 Photos of reproduced night light of scaled city of Turin (left), and the images taken by Mini-EUSO Engineering Model in TurLab measurement, superposed every 10 D3 GTUs across the entire city and its suburbs (right). The tank rotation speed for this run corresponds to three times faster than the one corresponding to Mini-EUSO. Bottom: A light pollution map of Nur-Sultan, one of a cities observed by Mini-EUSO (left), and the image taken by Mini-EUSO. Red square indicates Mini-EUSO FoV, each major city indicated in the pollution map or the photo of Turin city in TurLab with Alphabet corresponds to Mini-EUSO PDM image on the right. Image adapted from [31]

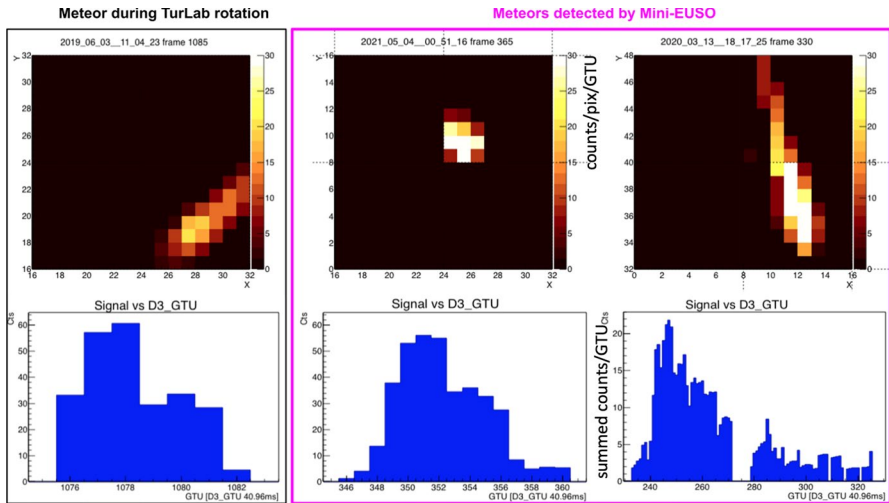


Fig. 14 Left: The image of a meteor event reproduced in the TurLab measurement during tank rotation which is passing by through a MAPMT (top) and its time evolution (bottom) as a function of D3 GTU (40.96 ms). Middle and Right: Examples of meteor events detected by Mini-EUSO. Integrated images (top) and time evolution plots (bottom). The blank part in the time evolution plot on the right is due to the gap between 2 MAPMTs where meteor is passing through. Image adapted from [31]

Therefore, these results on diffuse light sources are representative also in view of the future large missions K-EUSO and POEMMA which have similar apertures and instantaneous FoV.

Another important comparison is on the spatial extension and temporal durations of localized light emissions, either emitted or diffused lights, performed at TurLab to check for similarities with Mini-EUSO observations. The temporal duration of light sources is flexible by rotating the tank at different speed. Figures 13 and 14 provide direct comparisons of city lights and meteors. Figures 15 and 16, show some examples of localized light sources generated at TurLab with different solutions (i.e. sand, cloud or meteor). Mini-EUSO equivalent observations are shown in Figs. 17 and 18. A specific and more quantitative comparison for some typology of signals is provided in the following.

4.2 City lights

A first comparison is done with city lights. One example is provided in Fig. 13. Top part shows the representation of Turin city and surroundings at TurLab. This situation is compared with images taken by Mini-EUSO on Nur-Sultan (Astana), the capital city of Kazakhstan (bottom part). From population and altitude point of view, Nur-Sultan is similar to Turin (~1 million people for both, located at 347 m and at 239 m respectively), however, the area is 3 times bigger. It has also full of golden buildings, enormous shiny objects and even bright laser illuminating the sky

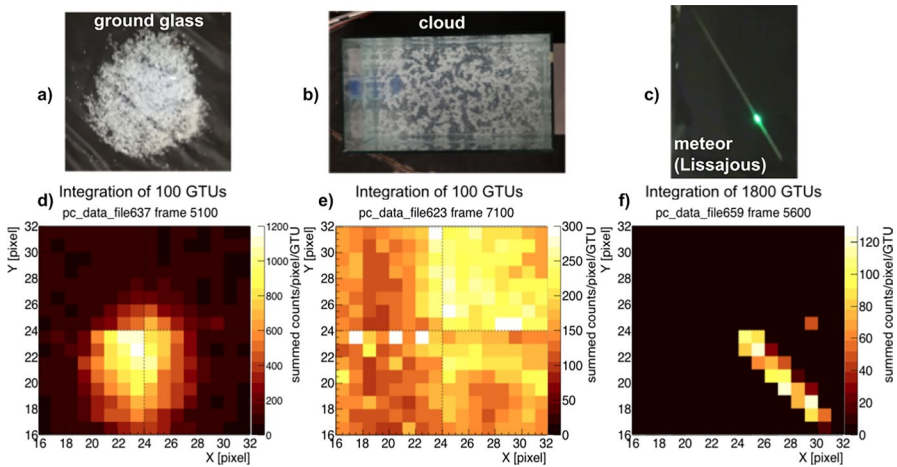


Fig. 15 Top: Examples of UV images obtained by the EC unit (2×2 MAPMTs, phase 2) passing by the various materials during the full tank rotation (~ 9 min to be in the range of suitable speeds for Mini-EUSO comparisons, see Table 2): a) city light is emulated by a ground glass illuminated by an LED; b) cloud is emulated using particles suspended in water; c) meteor track is reproduced using an analog oscilloscope. Bottom: the three plots in d) - f) show the corresponding images of a) - c) obtained during each event and integrated during the indicated number of D1 GTUs. It is important to remind that there is a difference in the spectra between the real physical sources and the simulated ones at TurLab. However, what matters is the similarity of the extension of the imaged signal and of the count rates between TurLab and Mini-EUSO setups

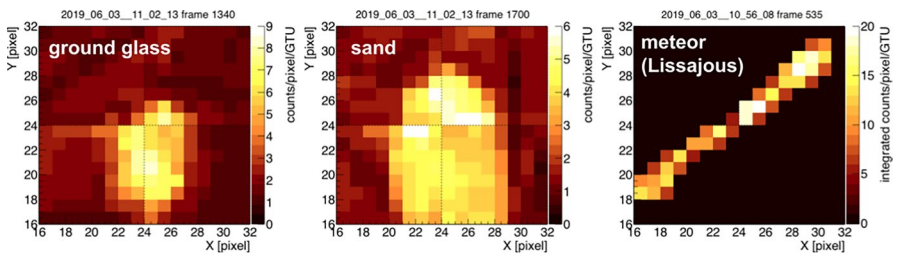


Fig. 16 Similar plots as in Fig. 15 but integrated over 1 D3 GTU which have been acquired during the third phase with the 41 ms time resolution available. In this run the meteor intensity is ~ 6 times dimmer (about two magnitudes higher) than the one displayed in Fig. 15

for decoration. Such a city has very similar profile to the representation of Turin city from the point of photo-electron counts and area.

Another example of city lights detected by Mini-EUSO is depicted in Fig. 17 and shows West Bengal in India. This is a densely inhabited region with the metropolis of Kolkata and other towns and villages in the area. In the Mini-EUSO FoV, the largest urban areas extend on an EC or a MAPMT scale, while smaller villages appear in groups of 2-4 pixels. This is similar to the transit of Turin map at TurLab. When Turin city is in the FoV, half EC is illuminated while small villages illuminate only few pixels.

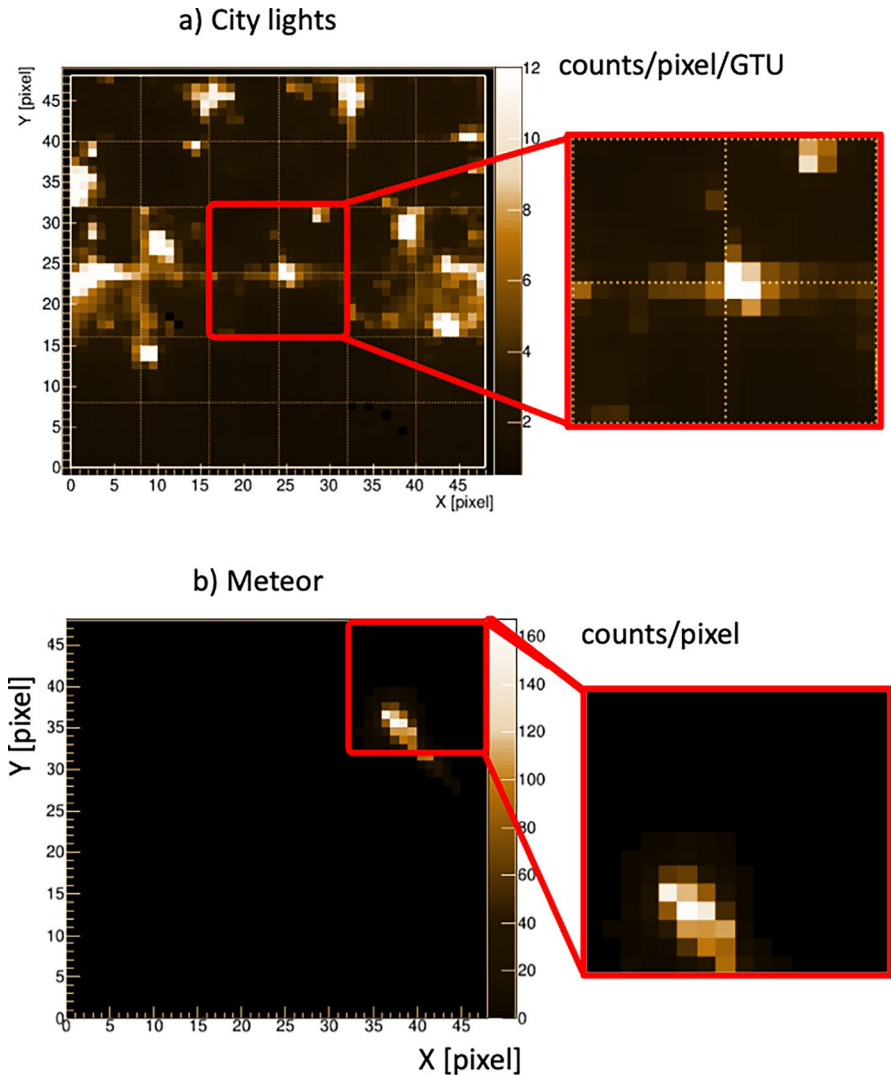


Fig. 17 Images taken by Mini-EUSO (figure adapted from [6]): a) one frame of $320 \mu s$ of an urban area on the East coast of India (West Bengal); b) a meteor track integrating over 41 ms time frames; For both plots, a zoom on a single EC scale of 16×16 pixels has been made for a better comparison with EUSO@TurLab images

In case of a much finer pixel FoV, like in JEM-EUSO, the spatial distribution would scale by a factor of 100 in area. Therefore, the EC-scale bright areas would correspond to 100 km^2 areas (like the city light reproduced using glass dust in Fig. 15) and localized bright spots to 1 km^2 areas.

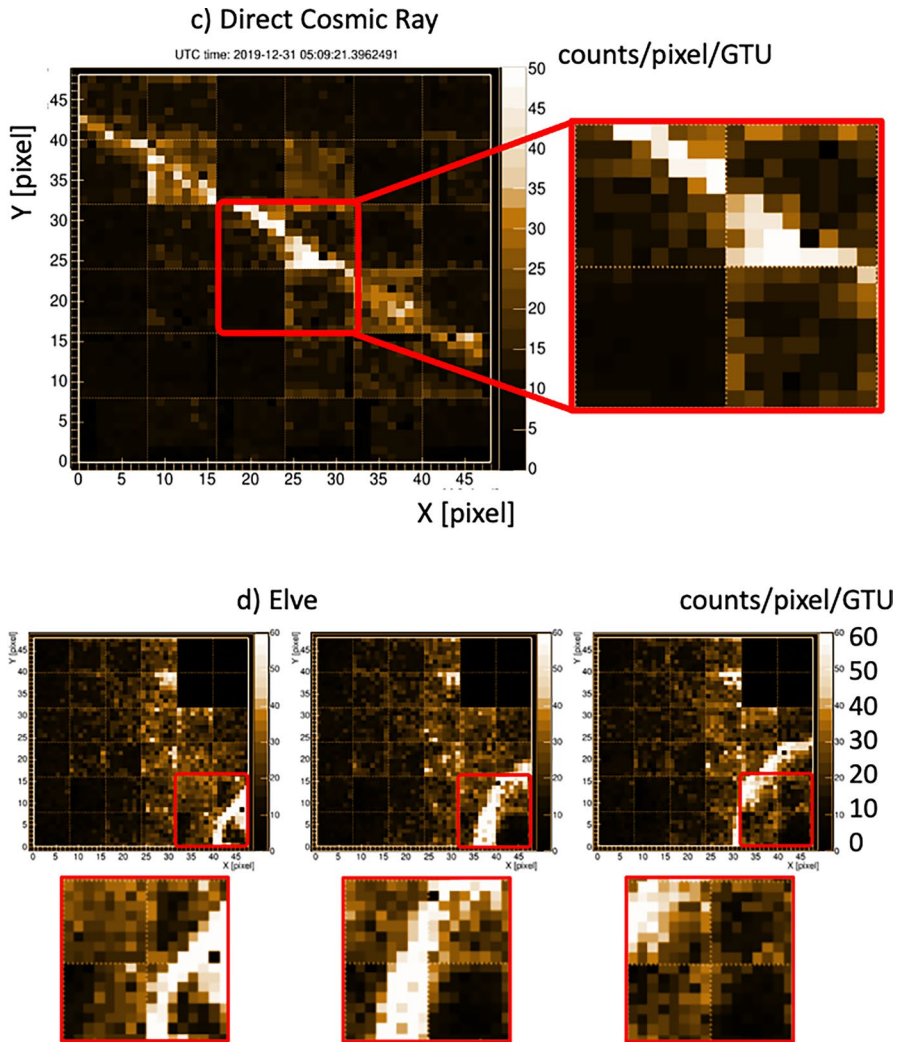


Fig. 18 Images taken by Mini-EUSO (figure adapted from [6]): c) a direct cosmic ray which hit the focal surface of Mini-EUSO almost parallel to it (the cosmic ray crosses the entire FS in one single frame of $2.5 \mu\text{s}$); d) time evolution of an ELVE where the three frames shown here have a duration of $2.5 \mu\text{s}$ each and are separated by $7.5 \mu\text{s}$. For both plots, a zoom on a single EC scale has been made for a better comparison with EUSO@TurLab images

From the point of view of the light intensity, plots in Figs. 13, 15 and 16 show that city lights are order of at least 10 times brighter compared to surroundings. This confirms the good representation of urbanized areas at TurLab. Regarding the speed at which images flow through the pixel's FoV, by adapting the rotation speed of the tank, it is possible to properly reproduce it for different space

experiments. In these comparisons the tank was rotated with a ~ 9 min period to be in the expected range of speeds which are comparable for Mini-EUSO (see Table 2).

4.3 Meteors

The first example of track events is shown in Fig. 14. The left plot shows a meteor track reproduced at TurLab while middle and right plots show two examples of detected meteors by Mini-EUSO with their light profiles. Other examples of meteor tracks at TurLab are shown in Fig. 15(f) and in Fig. 16. They last typically hundreds of ms up to a few seconds in case of very bright events. Figure 17(b) shows another very bright meteor seen by Mini-EUSO. The signal is ~ 100 times the nominal background level and it lasts for more than 1 sec (see Ref. [6] for details) and extends on 1 MAPMT. This is similar to what is shown in Fig. 15 in terms of spatial extension and contrast of luminosity but this depends on the magnitude of the meteor. By controlling the light intensity of the analog oscilloscope it is possible to change extension and duration of the signal. In fact the meteor shown in Fig. 16 has a much longer spatial extension even though it is ~ 10 times dimmer than the one shown in Fig. 17. This shows the variety of experimental events observed from space and their reproducibility at TurLab.

4.4 Flashers and cosmic rays

Another example of track-like events are EAS-like events. At TurLab an Arduino board controlling a line of 10 white LEDs is used to emulate a single EAS propagating through the atmosphere at the speed of light, resulting in a total duration of about 40 GTUs. As can be seen in Fig. 19, this signal no longer stays within one pixel during 10 GTUs, with the center of light moving clearly between subsequent GTUs.

Since Mini-EUSO has an energy threshold above 10^{21} eV, it is very unlikely to detect EECRs. However, direct cosmic rays can interact in the detector and generate EAS-like tracks but with a much shorter duration (1 GTU). An example of such a direct cosmic ray is shown in Fig. 18. Similar events could be reproduced at TurLab by extending the LED strip and switch on at the same time all the LEDs. The light intensity of 50 counts/pixel/GTU matches the experimental measurements as shown in the right-bottom plot of Fig. 19, even though here the LEDs are switched on at subsequent times. This is a class of events that is producing in JEM-EUSO detectors much brighter signals than expected. In fact, it was considered that the single photon counting technique coupled with a few ns double pulse resolution would have mitigated the luminosity of the light signals, assumed to be instantaneous. For this reason, this kind of events was not set up at EUSO@TurLab project but it could be easily reproduced in future tests. However, the experimental evidence of such events in flight suggests that the decaying times of direct ionization of cosmic rays in the photocathode and in the glass filter are much longer than the double pulse resolution, lasting at least one GTU.

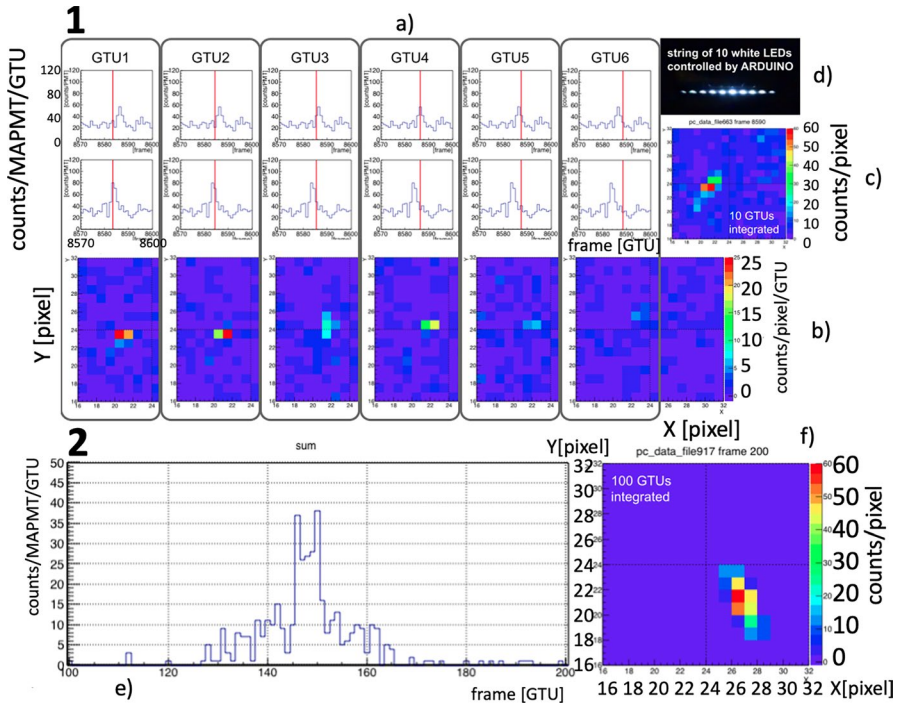


Fig. 19 Reproduction of EAS-like tracks at TurLab in the second phase. Part 1 of the figure shows in 1-a) for 6 GTUs the same light sequence (total counts on 1 MAPMT as a function of $2.5 \mu\text{s}$ GTUs) obtained by illuminating the FoV of the MAPMT with the Arduino-driven LED sequence shown in 1-d). In these 6 panels the total number of counts on one MAPMT is displayed with a red line indicating the specified GTU. The bottom 6 plots (1-b) show the corresponding images at MAPMT level. The 10 GTU integrated image is displayed in 1-c). The average background level is set at ~ 0.5 counts/pixel/GTU. Part 2 of the figure shows for another Arduino-driven event the integrated counts during the event in 2-e) and the full light track in 2-f). In this case no background light is present. Figure adapted from [29]

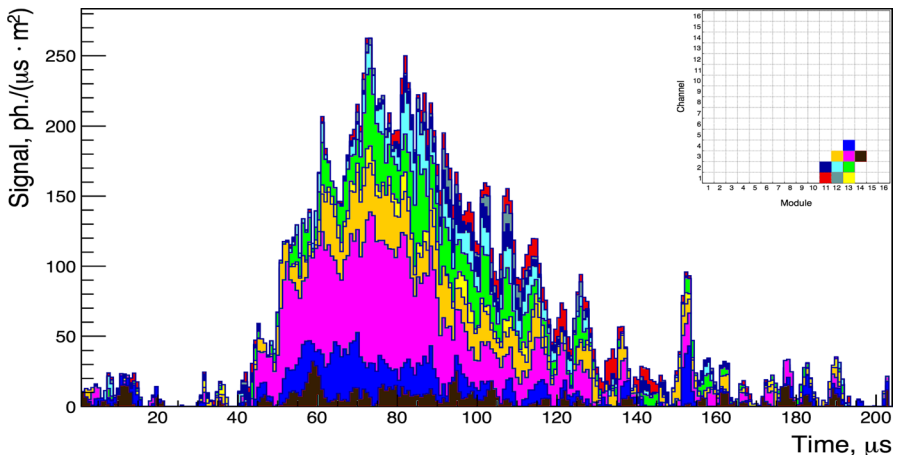


Fig. 20 The light curve of the TUS161003 event as the signal of the ten hit channels stacked together. The insert shows the positions of the hit pixels in the focal surface. Figure adapted from [33]

Another example of localized and fast flash comes from the TUS mission and it is shown in Fig. 20. According to [33] the event is measured in perfect observation conditions, with clear atmospheric conditions and no extended anthropogenic light sources in the vicinity, as an ultraviolet track in the nocturnal atmosphere of the Earth. The most plausible interpretation of the event implies its anthropogenic nature. However, it is not possible to rule out other origin of the event [33]. As no clear EAS track has been seen from space by the experiments of the JEM-EUSO program, aside from simulated events with ESAF (see Fig. 1), we use this experimental event for comparisons with TurLab measurements of EAS tracks, as this specific event shows some similarities in terms of kinematics and light curve with those expected from an EAS. The energy of the event is reconstructed to be of the order of 10^{21} eV if EAS simulations are used to assign an equivalent energy [33]. In this case the event appears to have a duration comparable to the TurLab event displayed in the bottom part of Fig. 19 having both a $\sim 100 \mu$ s duration. However, the reconstructed energy of the TUS event is extremely high and the LED intensities of the Arduino circuit at TurLab do not match it. The Arduino circuit is currently tuned to emit comparable light intensities with expectations from EECRs simulations in the 10^{20} eV region for the JEM-EUSO detector. They are also comparable with expectations for Mini-EUSO in case of 10^{22} eV EECRs (see Fig. 12).

4.5 Lightning and TLEs

Another dominant category of events seen from space is lightnings and TLEs. They represent a wide class of different phenomena on variable time scale and spatial extension ranging from a few kilometers to hundreds of kilometers like in the case of ELVEs. Figure 21 shows three frames of an ELVE viewed by TUS. The event is generated outside the FoV and the ring develops within it. The event is short in time and fast in speed (order of the light-speed).

Figure 22 shows ~ 240 seconds of the Mini-EUSO data. Examples of lightnings are detected together with city lights and counts from uninhabited areas. In general, lightnings appear as spikes lasting tens or hundreds of milliseconds

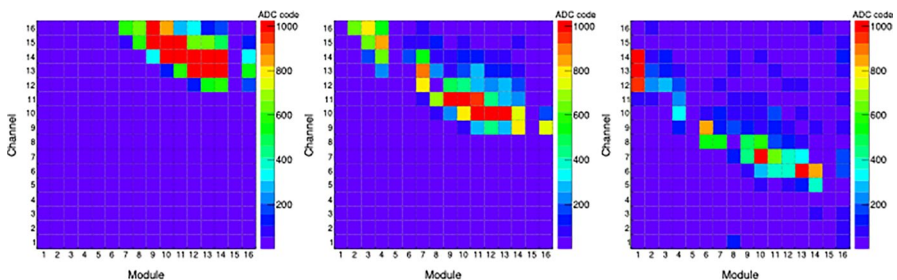


Fig. 21 Snapshots of the focal plane show the arc-like shape and movement of an image of the ELVE registered on 23 August 2017, through TUS detector's field of view. The snapshots were taken at 136μ s, 168μ s and 200μ s from the beginning of the record. Colors denote the signal amplitude in ADC codes. Figure taken from [5]

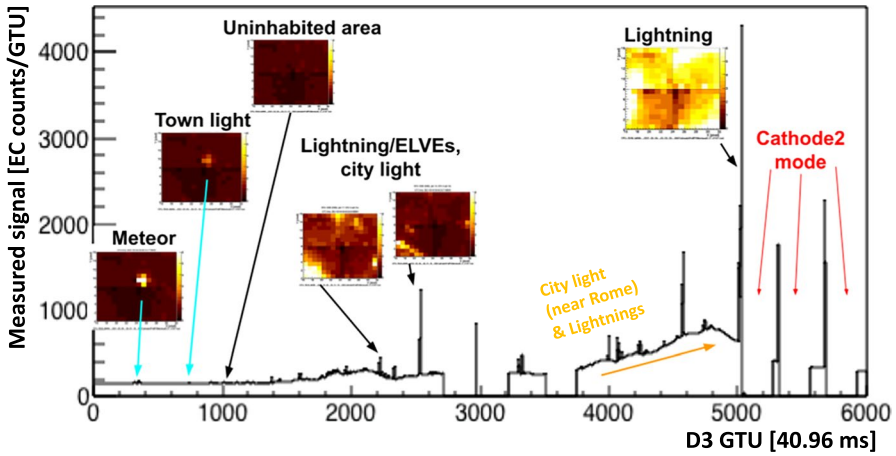


Fig. 22 An example of ~ 240 seconds of Mini-EUSO data with signals due to different sources: meteor, town and city lights, uninhabited areas, lightnings and ELVEs. At the end of the sequence the internal protection system is activated (Cathode 2 mode) and MAPMTs work at a reduced efficiency to avoid too large currents that could damage the MAPMTs. Each inset corresponds to a matrix of one EC (16 \times 16 pixels). Figure adapted from [31]

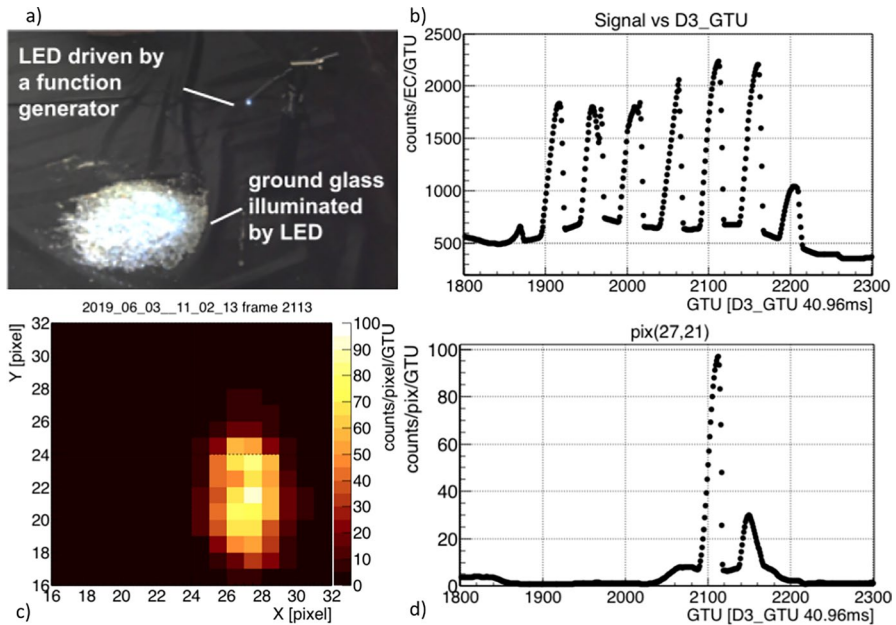


Fig. 23 At TurLab lightning are generated by illuminating glass dust with a white pulsed LED (a). The panel b) shows a train of the generated pulses during the motion of the tank, while c) displays the size of the event and d) a detail of one light pulse as seen by the pixel with the highest counts

depending on the location of the event and the signal increases by 1 - 2 orders of magnitude. They are seen only in portion of the FoV if happening outside it, or they can affect the entire FoV with different intensities if occurring within the viewing area, partly due to the scattering of the light by the optical system on the entire FS. If the lightnings are too intense the internal protection system is activated (Cathode 2 mode) and MAPMTs work at a reduced efficiency to avoid too large currents that could damage the MAPMTs. In this condition the count rate becomes almost negligible on uninhabitated areas.

As previously mentioned at TurLab lightnings are created by pulsing an LED on glass dust (see Fig. 23). The intensity shown here is an order of 100 times the background light level. The duration of the pulses is ~ 1 s but it can be controlled. The spatial extension of the signal seen by the camera is comparable to those of the experimental measurements. It can be noticed that depending on the position of the light source in the FoV, the entire MAPMT, or only a portion is illuminated, like in the Mini-EUSO detections.

As previously described at TurLab ELVEs are generated by means of an Arduino circuit that drives LED signals going through wavelength shifter fibers (see Fig. 24). The anular shape of the signal is comparable with the TUS and Mini-EUSO detected events. A direct comparison of the detected light intensity with TUS can not be done as the signal is not converted in photon intensity, however, it is in line to what is observed with Mini-EUSO (see Fig. 18). In Fig. 24 the images are taken in the first phase of the project, using a MAPMT with 25 pixels. With finer pixeling the image will look more spread out on the MAPMT.

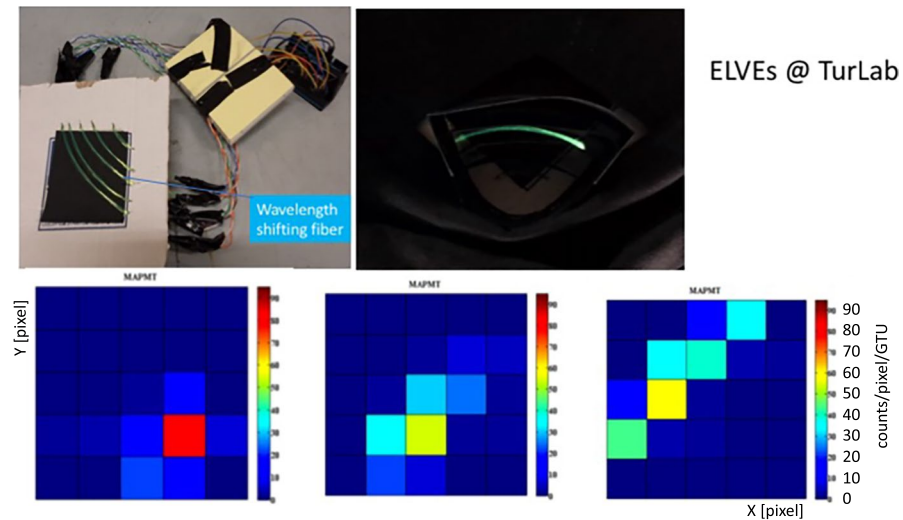


Fig. 24 At TurLab ELVEs are generated by means of an Arduino circuit that drives LED signals going through wavelength shifter fibers. By changing the temporal sequence of the switches, faster or slower events are created. Three frames of a sequence are plotted in the bottom part of the picture

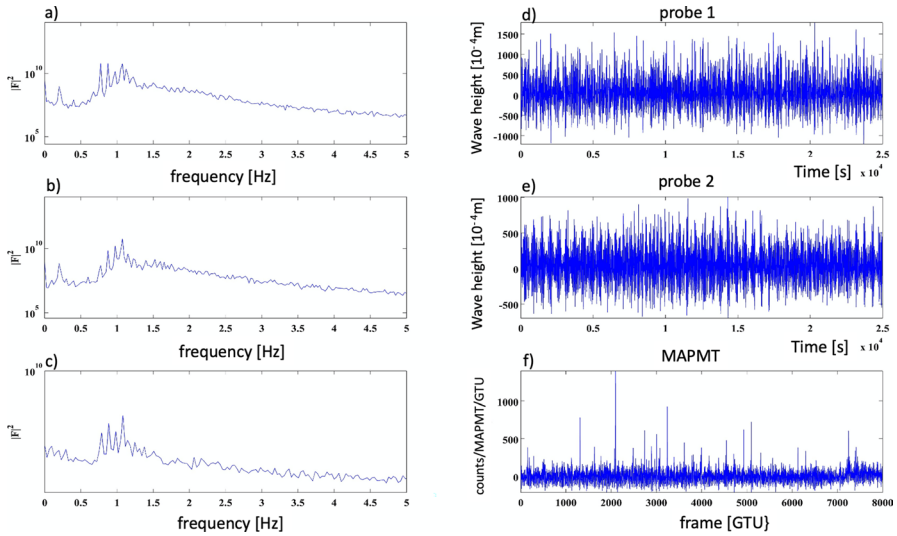


Fig. 25 Right side: the panels d) and e) show the wave heights measured with dedicated probes as a function of time. The panel f) show the MAPMT counts recorded at similar times due to the reflected light of a lamp illuminating the water. Left side: Fourier analysis of the plots on the right side. Both probes (a and b) and MAPMT intensities (c) show peaks at similar frequencies

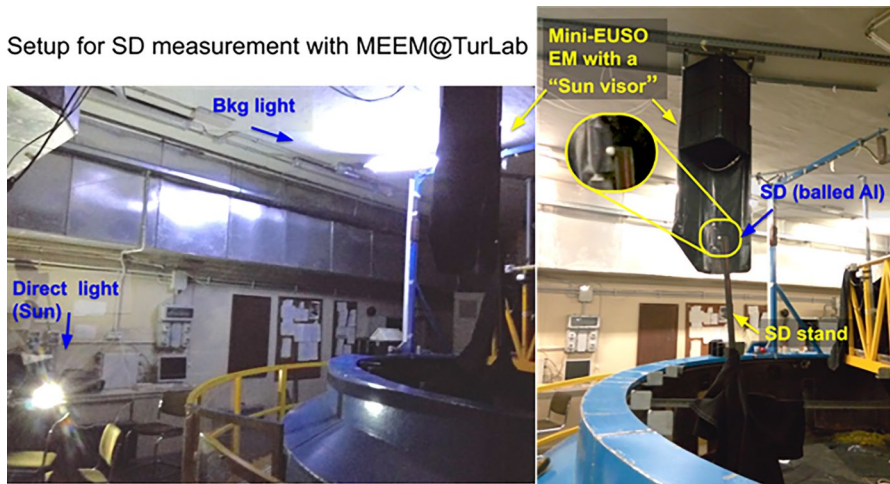


Fig. 26 TurLab setup for SD detection by the Mini-EUSO EM. The FS of Mini-EUSO EM apparatus is protected by a “Sun visor” to avoid the direct light from the white LED which is fixed outside of the tank, mimicking the Sun light. An Aluminum-ball under the apparatus of Mini-EUSO EM is attached to a solid stand which is fixed to the bottom of the tank. As the tank rotates, the Aluminum-ball moves within the EUSO@TurLab apparatus FoV being illuminated by the LED. Image adapted from [36]

5 Other applications

TurLab is a laboratory for geo-fluid-dynamics studies. Therefore, experiments related to this field are being conducted at TurLab within the EUSO@TurLab project. The response of the EUSO@TurLab apparatus is studied in presence of waves and/or foam inside the tank. A change in the UV reflection is observed if water contains patches of foam.

As a different branch of tests, a study of the effect of the reflection of light from waves is performed. A Fourier analysis of the wave amplitude and of the light intensities recorded by the EUSO@TurLab sensor show that peaks occur at the same frequencies (see Fig. 25). This indicates that the intensity of the light is correlated with the wave amplitude being related to the incident angle of the radiation onto the water surface. Higher amplitudes increase the chance that the water surface produces a specular surface that directly reflects part of the light to the sensor. This is responsible for the high MAPMT counts seen in the data such as around GTU 2000 in Fig. 25f.

The results of the two types of experiments here described might indicate that imaging experiments of the JEM-EUSO program could be sensitive to ocean phenomena. This can be tested by analyzing the data collected by Mini-EUSO in space. An example of the importance of such monitoring is related to whitecaps. They are a major source for wave energy dissipation and represent an important mechanism for air-sea exchange of gasses. Bubble bursting produces marine aerosols that contribute to climate regulation and whitecaps are reflector of light radiation responsible for increase of the albedo [34]. Even though whitecaps develop on spatial scales of tens of squared meters when waves are forced by the wind, as their wavelength is ~ 100 m, several whitecaps will be present in a pixel FoV of order of squared kilometers like in Mini-EUSO, thus it is expected that the sea albedo will increase and consequently the detected light intensity.

As the third miscellaneous application, at TurLab we tested the detection principle of space debris using the concept developed in [35]. It is based on an orbiting debris remediation system comprised of a super-wide field-of-view telescope (like JEM-EUSO) and a novel high-efficiency fiber-based laser system (CAN). The JEM-EUSO telescope detects the reflected light from a centimeter-sized space debris illuminated by moon or sun. The light comes from the back of the telescope, which is pointing to the deep sky. After tracking the debris thanks to its albedo for a while, a very powerful laser system would de-orbit it with laser pulses.

To verify this idea, we performed dedicated experiments at TurLab. Figure 26 shows the setup for reproducing SD detection principle. The apparatus of Mini-EUSO EM is hung on the ceiling above the TurLab tank, with a “Sun visor” to avoid the direct light from the high power LED which is emulating the Sun light. As the tank rotates, the ball moves within the FoV of the Mini-EUSO apparatus being illuminated by the LED (see Fig. 27), while the apparatus remains in the shade of the Sun visor. In such a way we could reproduce the SD detection.

Moreover, different materials (see bottom left Fig. 2), which often compose SD, are placed on the bottom of the tank, within the FoV of the EUSO@TurLab

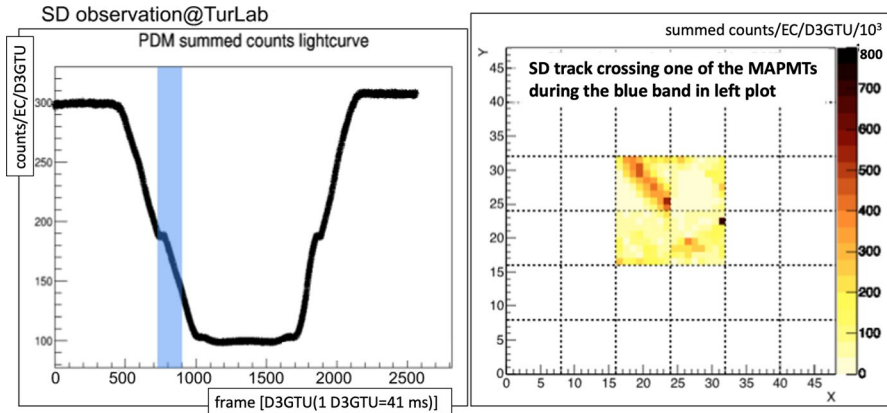


Fig. 27 Left side: Summed D3 data of all 4 MAPMTs as a function of D3 GTU during the Aluminum-ball passage back and forth through the Mini-EUSO EM FoV. The highest counts correspond to the position of the ball in the FoV which gives the highest count rate. The minimum corresponds to when the ball is outside the FoV. The total amount of counts varies during the passage through the FoV because of the different reflecting angle. Right side: A portion of the integrated track when the Aluminum-ball passes in the FoV of the top right MAPMT. This time span corresponds to the blue shaded area in the left plot

apparatus, in order to measure the relative reflectances of these materials. These results are used to estimate the sensitivity of Mini-EUSO and the other detectors of the JEM-EUSO program in recognizing SD. More details about these experiments and relative results about material reflectances and Mini-EUSO sensitivity to SD are reported in [36].

Finally, dedicated campaigns are performed using the EUSO-Balloon PDM recovered after flight to test the response of the trigger logic to be implemented in EUSO-SPB1 campaign, and using the Mini-EUSO EM as shown in Fig. 26. In case of EUSO-Balloon, the FLT logic is validated. The system that automatically adjusts the thresholds to keep the rate of triggers on background fluctuations below 1 Hz/EC even in case of slow background variations, is effective. The FLT detects EAS-like events with light intensities of ~ 20 counts/MAPMT/GTU, which are comparable to those JEM-EUSO would observe in the expected energy range ($E > 5 \times 10^{19}$ eV) and in presence of low nightsky background intensities ~ 0.2 counts/pixel/GTU. The FLT shows to be quite effective in rejecting city-like and lightning type of events. Only few spurious triggers occur [27].

Regarding the Mini-EUSO EM, aside from the SD test already mentioned, the data acquisition and control software are validated [37]. Tests performed on the FLT logic indicate that the trigger thresholds has to be increased compared to the originally planned ones to satisfy the required trigger rate on non standard background conditions such as in very low background environment or in presence of city lights [32]. Such stricter thresholds are currently employed in Mini-EUSO on the ISS [38], confirming the importance of the TurLab tests prior to instrument flight.

6 Conclusions and perspectives

The EUSO@TurLab project is an ongoing activity with the aim at reproducing in a laboratory environment the luminous conditions that a project of the JEM-EUSO program sees while flying in space. Along the years, the instrumentation at TurLab has evolved to re-create more and more settings. In parallel the electronics setup has improved by acquiring the same front-end electronics employed in the missions of the JEM-EUSO program to emulate as close as possible the real conditions. At the beginning the setup was fine tuned based on simulation results of how different phenomena, such as nightglow background, clouds, EAS-like events, meteor tracks, cities, lightings among others, were expected to be seen from space. Thanks to the Mini-EUSO and TUS missions it is now possible to compare past results with those obtained by real measurements. It is proven that the experiments at TurLab reproduce with a good reliability the phenomena seen from space in terms of spatial extension, duration and light intensities. This is important because it allows future tests of the electronics of the new missions of the JEM-EUSO program prior to flight and to use the TurLab as a facility to emulate flight observations. Moreover, it will be possible to test upgrades of the mission firmware prior to implement them on-board, saving resources and time for tests in space. The trigger logic of the EUSO-SPB1 and Mini-EUSO missions was deeply tested at TurLab. The good performance of the firmware of both instruments in flight is also merit of the variety of conditions that were tested with success at TurLab to emulate several environmental or/and luminous conditions that the telescopes would encounter. Finally, we tested the response of this kind of detectors for space debris observation and for marine and atmospheric science, that will be verified in space. They show the potential of JEM-EUSO sensors in these fields, and at the same time demonstrate the versatility of the tests that can be conducted at TurLab.

At present, the EUSO@TurLab apparatus is being upgraded and is being employed in the tests of the trigger logic of the EUSO-SPB2 mission [39]. In future it will be used to study the performance of new front-end electronics for SiPM detectors, which is currently under development for the measurement of both fluorescence and Cherenkov light emissions from EAS by space-based detectors (FluChe project [40]).

Acknowledgements This work has been partially funded by the Italian Ministry of Foreign Affairs and International Cooperation, by the European High-Performance Infrastructures in Turbulence (EuHIT), by Compagnia di San Paolo with the project “New techniques for the detection of space debris”; Id Project: CSTO164394, and from the agreement ASI-INAF n.2017-14-H.O. We thank the JEM-EUSO collaboration for supporting this initiative all along the different phases of the project and we acknowledge both JEM-EUSO and TUS collaborations for providing adapted plots of their results for a better comparison with TurLab experiments. The many constructive comments and suggestions of an anonymous referee to improve the clarity of the paper are deeply acknowledged.

Funding Open access funding provided by Università degli Studi di Torino within the CRUI-CARE Agreement.

Data Availability The datasets generated during and/or analysed during the current study are available from the corresponding authors on reasonable request.

Declarations

Conflict of Interests The authors declare that there is no conflict of interest.

Open Access This article is licensed under a Creative Commons Attribution 4.0 International License, which permits use, sharing, adaptation, distribution and reproduction in any medium or format, as long as you give appropriate credit to the original author(s) and the source, provide a link to the Creative Commons licence, and indicate if changes were made. The images or other third party material in this article are included in the article's Creative Commons licence, unless indicated otherwise in a credit line to the material. If material is not included in the article's Creative Commons licence and your intended use is not permitted by statutory regulation or exceeds the permitted use, you will need to obtain permission directly from the copyright holder. To view a copy of this licence, visit <http://creativecommons.org/licenses/by/4.0/>.


References

1. Bertaina M. for the JEM-EUSO Collaboration: An overview of the JEM-EUSO program and results. In: Proceedings of the 37th International Cosmic Ray Conference PoS(ICRC2021) 406 (2021)
2. Adams, J.H. Jr, et al.: (JEM-EUSO Coll.), Special Issue on The JEM-EUSO Mission. *Exp. Astron.* **40**, 1–326 (2015)
3. Füllekrug, M., Mareev, E.A., Rycroft, M.J.: *Sprites, Elves and Intense Lightning Discharges*. Springer, Berlin (2006)
4. De Rujula, A., Glashow, S.: Nuclearites—a novel form of cosmic radiation. *Nature* **312**, 734–737 (1984)
5. Klimov, P., et al.: (TUS Coll.), Remote sensing of the atmosphere by the ultraviolet detector TUS onboard the Lomonosov satellite. *Remote Sens.* **11**(20), 2449 (2019)
6. Bacholle, S., et al.: Mini-EUSO mission to study Earth UV emissions on board the ISS. *Astrophys. J. Suppl. S.* **253**(2) (2021)
7. Abdellaoui, G., et al.: (JEM-EUSO Coll.), EUSO-TA – First results from a ground-based EUSO telescope. *Astropart. Phys.* **102**, 98–111 (2018)
8. Adams, J.H. Jr., et al.: (JEM-EUSO Coll.), The EUSO-Balloon pathfinder. *Exp. Astron.* **40**, 281–299 (2015)
9. Wiencke, L., Olinto, A. for the JEM-EUSO Coll.: EUSO-SPB1 mission and science. In: Proceedings of the 35th International Cosmic Ray Conference, PoS(ICRC2017) 1097 (2017)
10. Adams, J.H., et al.: White paper on EUSO-SPB2. arXiv:1703.04513 (2017)
11. Klimov, P., et al.: (TUS Coll.), The TUS detector of extreme energy cosmic rays on board the Lomonosov satellite. *Space Sci. Rev.* **8**, 1687–1703 (2017)
12. Capel, F., et al.: (JEM-EUSO Coll.), Mini-EUSO: A high resolution detector for the study of terrestrial and cosmic UV emission from the International Space Station. *Adv. Space Res.* **62**, 2954–2965 (2018)
13. Klimov, P., et al.: (JEM-EUSO Coll.), Status of the K-EUSO orbital detector of ultra-high energy cosmic rays. *Universe* **8**, 88 (2022)
14. Olinto, A., et al.: (POEMMA Coll.), The POEMMA (probe of extreme multi-messenger astrophysics) observatory. *J. Cosmol. Astropart. Phys.* **2021**(6), 007 (2021)
15. Bertaina, M., et al.: (JEM-EUSO Coll.), EUSO@TurLab: An experimental replica of ISS orbits, Proceedings AtmoHEAD 2014. *EPJ Web of Conf.* **89**, 03003 (2015)
16. Aab, A., et al.: (The Pierre Auger Coll.), Measurement of the cosmic-ray energy spectrum above 2.5×10^{18} eV using the Pierre Auger Observatory. *Phys. Rev. D.* **102**, 062005 (2020)
17. Adams, J.H. Jr., et al.: (JEM-EUSO Collaboration), An evaluation of the exposure in nadir observation of the JEM-EUSO mission. *Astropart. Phys.* **44**, 76–90 (2013)

18. Berat, C., et al.: Full simulation of space-based extensive air showers detectors with ESAF. *Astropart. Phys.* **33**, 221–247 (2010)
19. Miyamoto, H., et al.: (JEM-EUSO Coll.), The EUSO@TurLab Project, Proceedings of the XXV European Cosmic Ray Symposium; preprint available at arXiv:[1701.07708](https://arxiv.org/abs/1701.07708) (2016)
20. Inan, U.S., Bell, T.F., Rodriguez, J.V.: Heating and ionization of the lower ionosphere by lightning. *Geophys. Res. Lett.* **18**, 705–708 (1991)
21. Pallavicini, M., et al.: The observation of extensive air showers from an Earth-orbiting satellite. *Astropart. Phys.* **35**, 402–420 (2012)
22. Adams, J.H., Jr., et al.: (JEM-EUSO Coll.), A review of the EUSO-balloon pathfinder for the JEM-EUSO program. *Space Sci. Rev.* **218**, 3 (2022)
23. Ferrero, E., et al.: Effect of rotation on buoyant plume dynamics. *Heat Mass Transf.* **58**, 1171–1185 (2022)
24. Piotrowski, L., et al.: (JEM-EUSO Coll.), Mini-EUSO data processing and quasi-real time analysis. In: Proceedings of the 35th International Cosmic Ray Conference PoS(ICRC2017) 373 (2017)
25. Caruso, R., et al.: (JEM-EUSO Coll.), The EUSO@TurLab project. In: Proceedings of the 34th International Cosmic Ray Conference PoS(ICRC2015) 674 (2015)
26. Kawasaki, Y., et al.: Performance of a multi-anode photomultiplier employing a weak electrostatic focusing system (Hamamatsu R8900 series). *Nucl. Inst. Meth. A* **564**(1), 378–394 (2006)
27. Suino, G., et al.: (JEM-EUSO Coll.), The EUSO@TurLab Project: Results from Phase II. In: Proceedings of the 35th International Cosmic Ray Conference, PoS(ICRC2017) 422 (2017)
28. Miyamoto, H., et al.: (JEM-EUSO Coll.), Performance of the EUSO-Balloon UV Camera. In: Proceedings of the Technology and Instrumentation in Particle Physics conference, PoS(TIPP2014) 362 (2014)
29. Abdellaoui, G., et al.: (JEM-EUSO Coll.), Cosmic ray oriented performance studies for the JEM-EUSO first level trigger. *Nucl. Instr. Meth. A* **866**, 150–163 (2017)
30. Miyamoto, H., et al.: (JEM-EUSO Coll.), The EUSO@TurLab: Test of Mini-EUSO Engineering Model. In: Proceedings of the 36th International Cosmic Ray Conference, PoS(ICRC2019) 194 (2019)
31. Miyamoto, H., et al.: (JEM-EUSO Coll.), EUSO@TurLab project in view of Mini-EUSO and EUSO-SPB2 missions. In: Proceedings of the 37th International Cosmic Ray Conference, PoS(ICRC2021) 318 (2021)
32. Bisconti, F., et al.: Pre-flight qualification tests of the Mini-EUSO telescope engineering model. *Exp Astron.* **53**, 133–158 (2021)
33. Khrenov, B.A., et al.: (TUS Coll.), An extensive-air-shower-like event registered with the TUS orbital detector. *J. Cosmol. Astropart. Phys.* **2020**(3), 033 (2020)
34. Anguelova, M. D., Webster, F.: Whitecap coverage from satellite measurements: A first step toward modeling the variability of oceanic whitecaps. *J. Geophys. Res.* **111**, C03017 (2006)
35. Ebisuzaki, T., et al.: Demonstration designs for the remediation of space debris from the International Space Station. *Acta Astronaut.* **112**, 102–113 (2015)
36. Miyamoto, H., et al.: (JEM-EUSO Coll.), Space Debris detection and tracking with the techniques of cosmic ray physics. In: Proceedings of the 36th International Cosmic Ray Conference, PoS(ICRC2019) 253 (2019)
37. Capel, F., et al.: Mini-EUSO data acquisition and control software. *J. Astron. Telescopes Instrum. Syst* **5**(4), 044009 (2019)
38. Battisti, M., et al.: Onboard performance of the level 1 trigger of the Mini-EUSO telescope. *Adv. Space Res.* **70**, 2750–2766 (2022)
39. Filippatos, G., et al.: Development of a cosmic ray oriented trigger for the fluorescence telescope on EUSO-SPB2. *Adv. Space Res.* **70**, 2794–2803 (2022)
40. Catalano, O., et al.: FluChe: Fluorescence and Cherenkov light detection with SiPM for space and ground applications. *Mem. S.A.It.* **93 N.2–3** (2022)

Publisher's note Springer Nature remains neutral with regard to jurisdictional claims in published maps and institutional affiliations.

Authors and Affiliations

P. Barrillon^{1,2} · M. Battisti^{3,4} · A. Belov⁵ · M. Bertaina^{3,4}  · F. Bisconti^{3,4} · S. Blin-Bondil^{6,7} · R. Bonino^{3,4} · F. Capel^{8,9} · R. Caruso^{10,11} · M. Casolino^{12,13} · G. Contino^{10,11,14} · G. Cotto^{3,4} · S. Dagoret-Campagne¹ · F. Fenu^{3,4} · C. Fornaro¹⁵ · R. Forza^{3,4} · P. Gorodetzky¹³ · N. Guardone^{10,11} · A. Jung^{7,16} · P. Klimov⁵ · M. Manfrin^{3,4} · L. Marcelli¹² · M. Mignone^{3,4} · H. Miyamoto^{3,4} · R. Mulas^{3,4} · M. Onorato^{3,4} · E. Parizot⁷ · L. Piotrowski^{13,17} · Z. Plebaniak^{3,4} · G. Prevot⁷ · J. Szabelski¹⁸ · G. Suino^{3,4} · Y. Takizawa¹³ · P. Tibaldi^{3,4} · C. Vigorito^{3,4} · A. Youssef^{3,4}

✉ M. Bertaina
marioeodoardo.bertaina@unito.it; bertaina@to.infn.it

✉ H. Miyamoto
hiroko.miyamoto@to.infn.it

- ¹ Université Paris-Saclay, CNRS/IN2P3, IJCLab, Orsay, France
- ² CPPM; CNRS/IN2P3, Aix-Marseille University, Marseille, France
- ³ Dipartimento di Fisica, Università degli Studi di Torino, Turin, Italy
- ⁴ INFN Sez. Torino, Turin, Italy
- ⁵ Skobeltsyn Institute of Nuclear Physics, Lomonosov Moscow State University, Moscow, Russia
- ⁶ Omega, Ecole Polytechnique, CNRS/IN2P3, Palaiseau, France
- ⁷ APC, Univ Paris Diderot, CNRS/IN2P3, Paris, France
- ⁸ KTH Royal Institute of Technology, Stockholm, Sweden
- ⁹ Technical University of Munich, Excellence Cluster ORIGINS, Garching, Germany
- ¹⁰ Dipartimento di Fisica ed Astronomia, Università di Catania, Catania, Italy
- ¹¹ INFN Sez. Catania, Catania, Italy
- ¹² Istituto Nazionale di Fisica Nucleare, Sezione di Roma Tor Vergata, Rome, Italy
- ¹³ RIKEN, Wako, Japan
- ¹⁴ INAF - IASF Palermo, Palermo, Italy
- ¹⁵ International Telematic University Uninettuno, Rome, Italy
- ¹⁶ Peking University, Beijing, China
- ¹⁷ Particles and Fundamental Interactions Division, Institute of Experimental Physics, University of Warsaw, Warsaw, Poland
- ¹⁸ National Centre for Nuclear Research, Lodz, Poland